DOCTORAL DISSERTATION SERIES

PUBLICATION: 5696

AUTHOR: Hans Peter Liepman, Ph. D., 1953
University of Michigan

TITLE: AN ANALYTIC DESIGN METHOD FOR A TWO-DIMENSIONAL ASYMMETRIC CURVED NOZZLE

University Microfilms, Ann Arbor, Michigan, 1953

AN ANALYTIC DESIGN METHOD FOR A TWO- DIMENSIONAL ASYMMETRIC CURVED NOZZLE

by
Hans Peter Liepman

A dissertation submitted in partial fulfillment
of the requirements for the degree of
Doctor of Philosophy in the
University of Michigan
1953

Committee in charge:

Assistant Professor John R. Sellars, Chairman
Associate Professor Robert C. F. Bartels
Professor Arnold M. Kuethe
Professor Wilbur W. Nelson
Associate Professor Julius D. Schetzer

AN ANALYTIC DESIGN METHOD FOR A TWO-DIMENSIONAL ASYMMETRIC CURVED NOZZLE

by Hans Peter Liepman

An analytic method is presented for the design of two-dimensional asymmetric curved nozzles. Such nozzles are of interest to designers of supersonic test facilities since they can achieve continuously varying Mach numbers by relative translation of one contour with respect to the other. Since such nozzles can also be designed without discontinuities in their wall curvatures, they have many desirable features. The only known method of designing this type of nozzle has been the graphical one of characteristics. Since it is shown that a graphical method is not accurate enough to assure the high quality of uniform flow desired in the test section, the need for an analytic design method is apparent.

The continuity equation and the condition of irrotationality for steady compressible flow are given in curvilinear co-ordinates with stream function and velocity potential as independent variables. Using Bernoulli's equation for an isentropic gas and a suitably chosen analytic velocity distribution along the initial expansion contour, which is specified in terms of its curvature, a set of partial differential equations is obtained. These equations are solved by expanding the dependent variables - velocity q, flow direc-

tion θ , and curvilinear co-ordinates (x, y) of a stream-line - in powers of the stream function. This solution determines the nozzle contours for any constant value of the stream function as well as all flow characteristics in the subsonic region and the supersonic expansion region of the nozzle. After the patching Mach line is calculated numerically the recompression contour can be determined to complete the nozzle calculations. The effect of curvature of the initial expansion contour on the flow near the throat, the patching Mach line, and the test section juncture is immediately apparent since the first order terms of the curvature parameter appear in the equations.

The actual application of this analytic method is then carried out for the design of a perfect fluid contour for a design Mach number of 2.37.

The variation of Mach number by relative translation of fixed contours of the asymmetric type is then discussed. An iteration method is derived for this purpose which should converge very rapidly as compared to the iteration required by the characteristics method of design.

Finally the problem of boundary layer corrections to this type of nozzle is reviewed. A criterion is suggested to determine if viscous corrections are needed or not. The actual process of carrying out such corrections is also indicated.

ACKNOWLEDGMENTS

The author wishes to acknowledge the encouragement, helpful suggestions, and guidance given by the individual members of his Committee. Appreciation is also extended to his former co-worker, Dr. James S. Murphy, now with Douglas Aircraft Company, for many valuable discussions of the problem.

Grateful acknowledgment is also extended to the Flight Research Laboratory, Wright Air Development Center, U. S. Air Force. This organization sponsored an experimental research project at the University of Michigan on a corner nozzle. This thesis, though entirely separate from the project, was directly motivated by it.

TABLE OF CONTENTS

	Page
LIST OF FIGURES	vi
NOTATION	vii
SUMMARY	1
CHAPTER I. INTRODUCTION AND MOTIVATION	3
1. The Asymmetric Curved Nozzle - Principle and Advantages	3
2. Design Methods for Asymmetric Nozzle Contours	6
3. Accuracy of Nozzle Calculations and Non-Uniformities in Test Section Flow	7
a) Effect of Contour Deviations on Test Section Flow	7
b) Design Tolerances for Nozzle Contours .	9
4. Review of Analytic Design Methods for Symmetric Nozzles	14
CHAPTER II. PERFECT FLUID THEORY OF ASYMMETRICAL NOZZLE CONTOURS FOR A GIVEN EXIT MACH NUMBER .	16
1. Fundamental Equations in Curvilinear Co-ordinates	16
a) Co-ordinate Systems	16
b) Velocity Potential and Stream Function .	18
c) Transformation of Basic Equations . .	21
d) Bernoulli's Equation and Equation of State	28

Page

2. Solution of Differential Equations 31
3. Discussion of Solution 36
   a) Validity of Solution 36
   b) Special Boundary Conditions 40
4. Equation of Patching Mach Line 43
5. Initial Mach Number Distribution and Wall Curvature at the Patching Mach Line . . . 47
6. Calculation of Patching Mach Line 49
   a) Runge-Kutta Method 50
   b) Series Approximation 52
7. Calculation of Simple Wave Region 54
8. Outline of Complete Nozzle Contour Calculations 56

CHAPTER III. NOZZLE CONTOUR CALCULATIONS FOR AN EXIT MACH NUMBER OF 2.37 60

1. Introduction 60
2. Basic Data 60
   a) h_o-Function 60
   b) Curvature Distribution 65
   c) Scale Factors 67
3. Nozzle Contours 68
   a) Subsonic and Supersonic Regions up to the Patching Mach Line 68
   b) Patching Mach Line 68
   c) Recompression Contour 76
   d) Complete Nozzle Contour 76

Page

CHAPTER IV. DESIGN MACH NUMBER CHANGE THROUGH CONTOUR TRANSLATION 78

CHAPTER V. BOUNDARY LAYER CORRECTION METHODS . . 85

1. Introduction 85

2. A Criterion for the Application of Boundary Layer Corrections 86

3. Boundary Layer Corrections for Asymmetric Curved Nozzles 90

APPENDIX A. TWO-DIMENSIONAL EQUATION OF CONTINUITY AND CONDITION OF IRROTATIONALITY IN CURVILINEAR CO-ORDINATES 93

APPENDIX B. CALCULATION OF COEFFICIENTS OF η-SERIES 97

APPENDIX C. SERIES OF EXPANSION OF DIFFERENTIAL EQUATION OF PATCHING MACH LINE 104

BIBLIOGRAPHY 107

LIST OF FIGURES

Figure		Page
1.1	Sketch of Asymmetric Curved Nozzle	4
1.2	Expansion and Compression Waves from a Contour Defect	8
1.3	Contour Deviations for Unit Percent Error in Test Section M, C_F, and p versus M	10
2.1	Curvilinear Co-ordinates	17
2.2	Differential Geometry in Curvilinear Co-ordinates	19
2.3	Velocity and Flow Direction as Field Variables	21
2.4	Streamlines and Potential Lines in Flow Field	24
2.5	Variables and Parameters of Curved Nozzle . .	37
2.6	Patching Mach Line	45
2.7	Recompression Region	55
3.1	Given h_o and h_o' Functions	62
3.2	Given h_o'' and h_o''' Functions	63
3.3	Mach Number Distribution along Lower Contour	64
3.4	Curvature Distribution of Lower Contour . .	66
3.5	x Co-ordinate for Upper Contour	69
3.6	y Co-ordinate for Upper Contour	70
3.7	Upper to Lower Wall Pressure Ratio	71
3.8	Speed Ratio along Upper Contour	72
3.9	Flow Direction along Upper Contour	73
3.10	η -Terms of Patching Mach Line Equation . .	74
3.11	Patching Mach Line Equation	75
3.12	Calculated and Comparison Nozzle Contours .	77

4.1 Relation Between Nozzle Translation and Design Mach Numbers 79
4.2 Nozzle Contours and h_o-Functions for One Iteration 83
5.1 δ^*-Slopes along Nozzle Contours 88
5.2 Boundary Layer Corrections 92

A-1 Mass Flux Through Incremental Area 96
A-2 Velocity Components along Incremental Area . . 96

NOTATION

A	Channel area (one-dimensional theory)
A^*	Critical Channel Area (sonic state)
C_F	Aerodynamic Force Coefficient
c	Speed of sound
H	Stagnation Pressure
h	Area Ratio Parameter
h_o	Area Ratio Parameter along Reference Contour
h_{oD}	Design value of h_o in Test Section
J	Jacobian
l	Length of left running characteristic in recompression region
M	Mach number
M_o	Mach Number along Reference Contour
M_D	Design Mach Number in Test Section
N	Number of Reflections of Disturbance Waves
n	Arc length along potential line
p	Static pressure
p_o	Static pressure along Reference Contour
P_E	Nozzle Exit Pressure
q	Resultant velocity
q^*	Critical (sonic) velocity
q_o	Velocity distribution along Reference Contour
q_1, q_2, q_3	Coefficients of q-series
R	Radius of Curvature of Reference Contour
s	Arc length along streamline
t	Test Section Height

u Velocity component in curvilinear x-direction

v Velocity component in curvilinear y-direction

X Cartesian Abscissa

Y Cartesian Ordinate

x Curvilinear Abscissa (along Reference Contour)

x_1, x_2, x_3 Coefficients of x-series

y Curvilinear Ordinate (normal to Reference Contour)

y_1, y_2, y_3 Coefficients of y-series

α Mach Angle

γ Ratio of specific heats

δ h_o-perturbation function

δ^* Boundary Layer Displacement Thickness

ϵ Angle between neighboring radii of curvature

η Independent variable, proportional to stream function

η_c Design value of η on upper contour

Θ Flow direction measured from curvilinear abscissa (on Reference Contour)

$\Theta_1, \Theta_2, \Theta_3$ Coefficients of Θ-series

κ Curvature ($=1/R$)

ξ Independent variable, proportional to potential function

ξ_D "Design" value of ξ at start of test section rhombus

ρ Density of gas

ρ_D Density of gas at design Mach number

ρ^* Critical density (Sonic State)

ψ Stream Function

ψ_D Stream Function for design contour

φ Potential Function

ω Slope of Reference Contour measured from Cartesian abscissa

Subscripts l and u refer to conditions on lower and upper nozzle contour, respectively.

SUMMARY

An analytic method is presented for the design of two-dimensional asymmetric curved nozzles. Such nozzles are of interest to designers of supersonic test facilities since they can achieve continuously varying Mach numbers by relative translation of one contour with respect to the other. Since such nozzles can also be designed without discontinuities in their wall curvatures, they have many desirable features. The only known method of designing this type of nozzle has been the graphical one of characteristics. Since it is shown that a graphical method is not accurate enough to assure the high quality of uniform flow desired in the test section, the need for an analytic design method is apparent.

The continuity equation and the condition of irrotationality for steady compressible flow are given in curvilinear co-ordinates with stream function and velocity potential as independent variables. Using Bernoulli's equation for an isentropic gas and a suitably chosen analytic velocity distribution along the initial expansion contour, which is specified in terms of its curvature, a set of partial differential equations is obtained. These equations are solved by expanding the dependent variables - velocity q, flow direction θ , and curvilinear co-ordinates (x, y) of a streamline - in powers of the stream function. This solution determines the nozzle contours for any constant value of the stream function as well as all flow characteris-

tics in the subsonic region and the supersonic expansion region of the nozzle. After the patching Mach line is calculated numerically the recompression contour can be determined to complete the nozzle calculations. The effect of curvature of the initial expansion contour on the flow near the throat, the patching Mach line, and the test section juncture is immediately apparent since the first order terms of the curvature parameter appear in the equations.

The actual application of this analytic method is then carried out for the design of a perfect fluid contour for a design Mach number of 2.37.

The variation of Mach number by relative translation of fixed contours of the asymmetric type is then discussed. An iteration method is derived for this purpose which should converge very rapidly as compared to the iteration required by the characteristics method of design.

Finally the problem of boundary layer corrections to this type of nozzle is reviewed. A criterion is suggested to determine if viscous corrections are needed or not. The actual process of carrying out such corrections is also indicated.

CHAPTER I

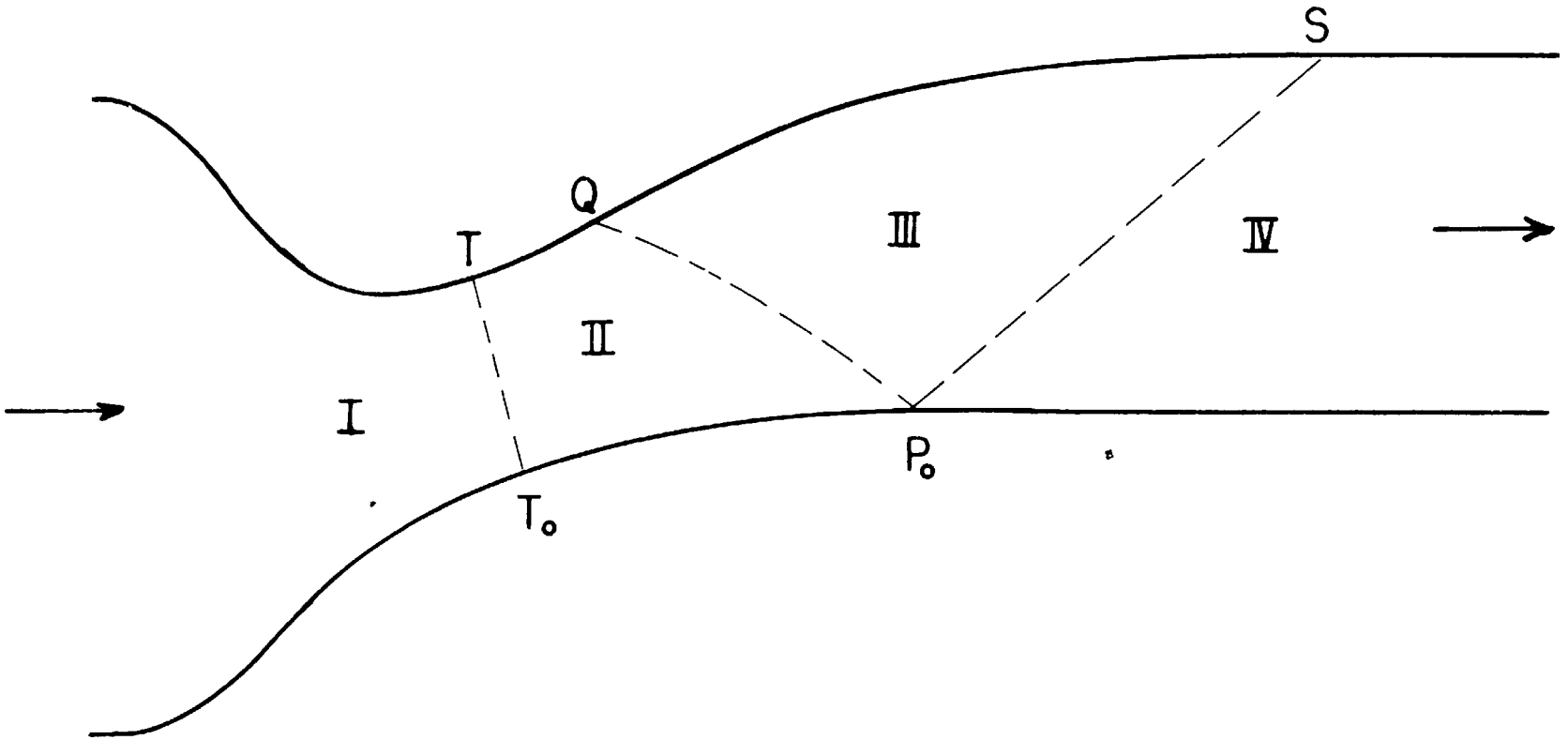
INTRODUCTION AND MOTIVATION

1. The Asymmetric Curved Nozzle - Principle and Advantages

The type of asymmetric curved nozzle under consideration is shown schematically in Figure 1.1. A suitable pressure differential between stagnation pressure H and exit pressure p_E draws air, or gas, through the nozzle. The air stream is accelerated first in the subsonic contraction region I and reaches sonic speed at the throat $T\text{-}T_o$. It accelerates supersonically in region II by expansion around the lower contour between T_o and P_o and reflection from the upper contour between T and Q. This flow region will therefore have characteristic curves of both left and right running families. Region II is terminated by region III, P_oQS, which consists of only left running characteristics. This last region cancels all excess expansions and turns the flow into a uniform, parallel, test section region, region IV, of the desired design Mach number.

Recent experimental work by the NACA has indicated that such a nozzle can be used to vary continuously the test section Mach number over a limited range. This is achieved by the relative translation of one contour with respect to the other parallel to the test section center line. The University of Michigan is presently carrying out a sponsored research project directed towards the extension of the Mach number range which such a nozzle can cover, and towards the

FIGURE 1.1



Sketch of Asymmetric Curved Nozzle

experimental determination of the nozzle contours resulting in most uniform test section flow.

The mechanical simplicity of translating one contour block with respect to the other to achieve a continuous variation in Mach number is the most outstanding feature of this nozzle and is of great interest to the designers of supersonic test facilities. Furthermore, potentialities exist with such a nozzle to simulate accelerated flight conditions by time-programming the nozzle translation.

The supersonic contours of an asymmetric nozzle can easily be made to have continuous wall curvature and thus avoid the difficulties associated with points of inflection and the nozzle-test section juncture occurring in conventional nozzles.

This type of nozzle will, of course, be about twice as long as a symmetrical nozzle; therefore there will be thicker wall boundary layers in the test region. The latter is not so serious as it may appear since no difficulties have been encountered from thick boundary layers during the many years of operation of the University of Michigan's 8" x 13" intermittent supersonic wind tunnel. This wind tunnel operates from atmospheric stagnation conditions and has its test section in the second design Mach rhombus (or about two symmetrical nozzle lengths downstream from the throat). The disadvantage of greater length and space requirements for an asymmetric nozzle are believed to be irrefutably outweighed by the advantage of the variable Mach number feature.

2. Design Methods for Asymmetric Nozzle Contours

At the present time only the graphical method of characteristics is available for the design of the contours of such an asymmetrically curved nozzle. This method also requires that the shape of the sonic line be assumed initially before the characteristic diagram can be started. For the design of the subsonic contour the only guidance available is the one-dimensional area theory which can be interpreted rather freely, especially in a curved channel.

In view of the results of the next section, the accuracy of a graphical method for the design of the nozzle contours is believed to be insufficient to assure acceptable uniformity of flow in the test section. Thus the need exists for an analytic method of design which can give the desired accuracy in the contour calculations. Such a design method is therefore developed from the most suitable nozzle design procedure for symmetric nozzles. This method has the further advantages that it does not require any assumption regarding the shape of the sonic line, and that it extends into the subsonic region.

Neither the method of characteristics nor the new analytic design method achieve the variable Mach number feature without a process of iteration. The iteration for the analytic design method appears to be considerably shorter than that for the characteristics method. Of course the high degree of numerical accuracy of the analytic method need not be lost in this iteration process.

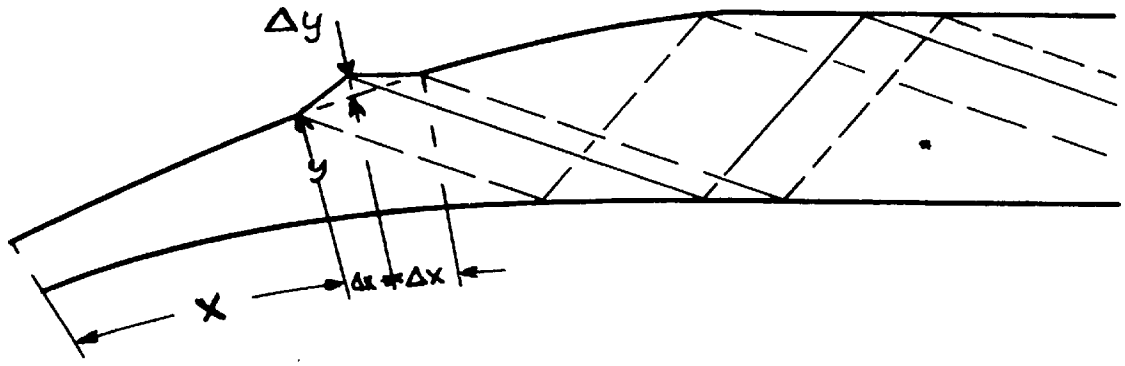
3. Relations Between Accuracy of Nozzle Contour Calculations and Non-Uniformities in the Test Section Flow

The analysis in this section relates the accuracy of nozzle contour computations to the percent error which can be tolerated in pressure, force coefficient, or Mach number in the test section. By use of the concept of infinitesimal disturbances (Mach waves) it is shown that an aerodynamically satisfactory nozzle is obtained only when its contours are calculated with a high degree of accuracy. An appropriate analysis indicates that nozzle ordinate calculations should be carried out to at least 4 significant decimal figures of unity. Such a degree of accuracy is usually unattainable by graphical means.

a) Effect of Contour Deviations on Test Section Flow

Let an error in contour ordinate of magnitude Δy occur at station x. This may be caused by an error in contour calculations or in fabrication. It may also be a waviness in the surface due to improper surface finish. Such an error will create a small wave; either expansion or compression which will ultimately reach the test section and give rise to a disturbance in Mach number and pressure field. The strength of this disturbance will depend on how often such a wave is reflected before it reaches the test section (Figure 1.2).

FIGURE 1.2



Expansion And Compression Waves From A Contour Defect

The effect of such a disturbance has been analyzed by Puckett for a symmetrical nozzle in Reference 1. He also gives the error in pressure, Mach number, and apparent force coefficient. The latter is derived from the assumption that the actual force coefficient is proportional to $(M^2 - 1)^{-1/2}$, and is

$$\frac{\Delta C_F}{C_F} = \left[\frac{(\gamma+1)M^2}{2\gamma(M^2-1)} - \frac{2}{\gamma M^2} \right] \frac{\Delta p}{p} \quad . \qquad (1.1)$$

For the case of an asymmetric curved nozzle the effect of contour deviations on pressure and Mach number errors was analyzed by Murphy and Buning (Reference 2) using Puckett's approach. The results are

$$\frac{\Delta y}{\Delta x} = \pm \frac{1}{N} \frac{(M^2-1)^{1/2}}{\gamma M^2} \frac{\Delta p}{p} \quad , \qquad (1.2)$$

and

$$\frac{\Delta y}{\Delta x} = \pm \frac{1}{N} \frac{(M^2-1)}{(1+\frac{\gamma-1}{2} M^2)} \frac{\Delta M}{M} \quad , \qquad (1.3)$$

where N is the number of reflections of a wave from a contour defect between the defect and the test section. Substitution of the pressure error equation (1.2) into the force coefficient error (1.1) gives

$$\frac{\Delta y}{\Delta x} = \pm \frac{1}{N} \frac{2(M^2-1)^{3/2}}{(\gamma+1)M^4 - 4(M^2-1)} \frac{\Delta C_F}{C_F} \quad , \qquad (1.4)$$

Equations (1.2), (1.3), and (1.4) are plotted in Figure 1.3 as $N\frac{\Delta y}{\Delta x}$ vs. test section Mach number for 1% changes in pressure, Mach number, and force coefficient. The results of this figure must be multiplied by allowable per cent errors different from 1 and divided by N for N≠1.

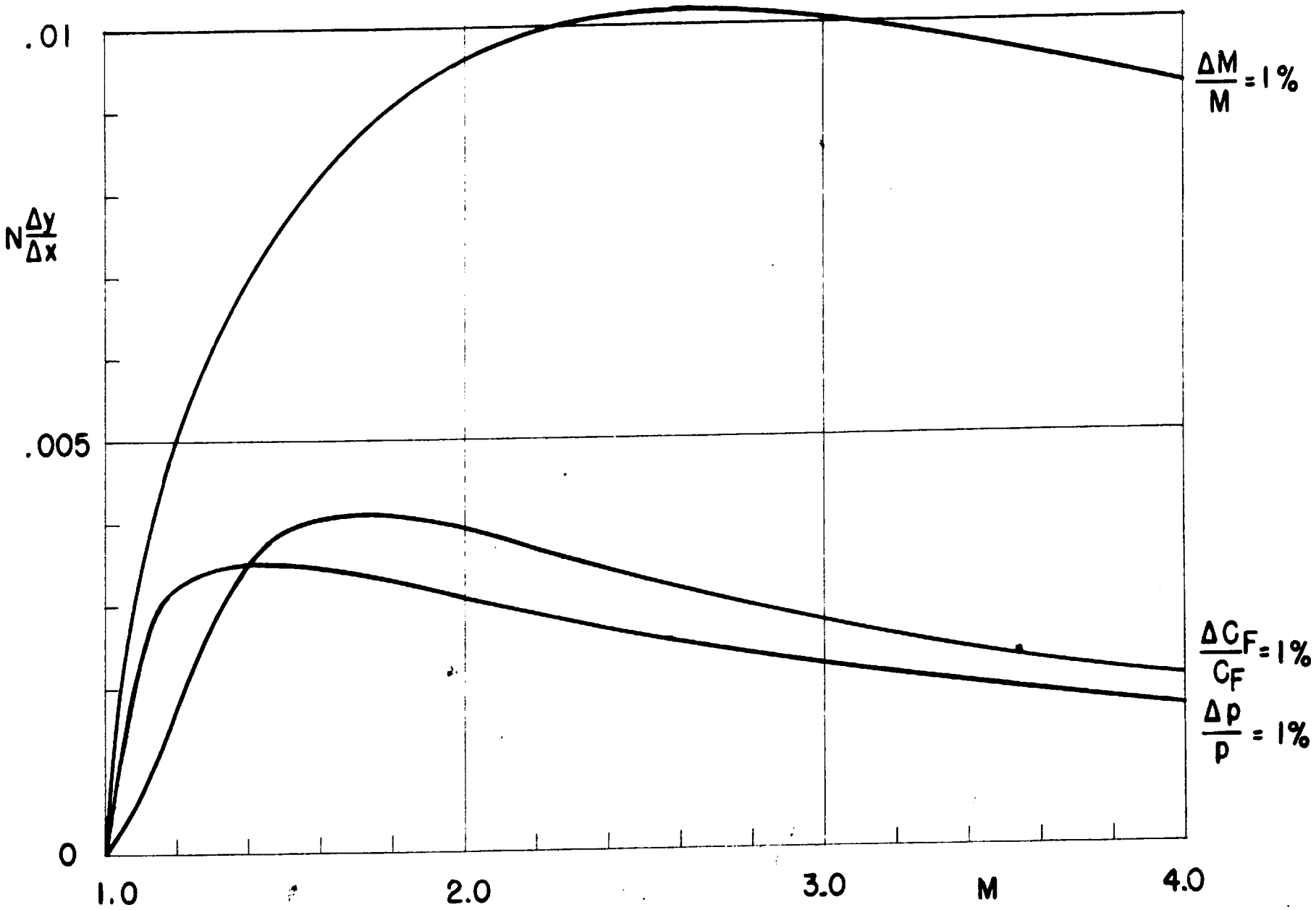
Attention is called to the fact that the slope of a Mach 4.0 nozzle near the exit (N=1) must be held to .10° to limit pressure and force coefficient errors to 1%. Near the throat, where N may be as high as 10, the nozzle slope must be held to .01°, a very stringent requirement.

b) Design Tolerances for Nozzle Contours

The design ordinates y_d of a supersonic nozzle are usually obtained from an analytical or graphical method and are given in terms of

FIGURE 1.3

Contour Deviations for Unit Percent Errors in Test Section M, C_F, & p vs. M



$$y_d = f(x) . \qquad (1.5)$$

For the construction of such a nozzle, manufacturing tolerances must be specified which are largely determined by economical considerations. Although these tolerances apply to both x and y values, the tolerance for the ordinate y is usually more critical. In the subsequent analysis only the manufacturing tolerance on y will be considered and will be denoted by $\pm \Delta y_m$. Hence the actual ordinate of a nozzle contour at a given axial station x will be

$$y = y_d \pm \Delta y_m . \qquad (1.6)$$

The design ordinate y_d is itself subject to a tolerance $\pm \Delta y_d$ which depends upon the accuracy of the method used to calculate the theoretical contours. Obviously Δy_d is quite large if a graphical design method is used. If an analytic method is used, Δy_d will depend upon the number of significant figures used in the calculations.

The actual contour of a nozzle can now be written as

$$y = y_d \pm \Delta y_d \pm \Delta y_m , \qquad (1.7)$$

and the maximum absolute value of $(\Delta y_d + \Delta y_m)$ should be equal to or less than the maximum error in contour which can be tolerated from the aerodynamic performance in the test section. The relations between aerodynamic errors and nozzle contour errors were given in part a) of this section.

In general it is found that the manufacturing tolerance Δy_m has a practical limit of 0.0005 inches. This limit applies not only to each individual contour ordinate y but also to any waviness tolerance. The latter is usually given in terms of allowable amplitude and frequency of a wave which, in turn, can be approximated in terms of Δy and Δx values.

The design tolerance Δy_d for a thorough graphical design method is probably about 0.001" or, at best, of the same order as the manufacturing tolerance. An analytic method, though, is capable of giving design tolerances of 0.0001" or better, depending upon the limits of the calculating machine used.

It is instructive to calculate the total ordinate error using $\Delta y_m = \pm .0005$, and $\Delta y_d = .001"$ and .0001", respectively, and to compare these errors with the resulting aerodynamic performance. For this purpose the above tolerances are considered maximum errors and are used as additive in the extreme case. Hence, the maximum error in the manufactured nozzle ordinate is

$$\Delta y = \Delta y_m + \Delta y_d \quad , \qquad (1.8)$$

or

$\Delta y = 0.00150"$ for graphical methods, and

$\Delta y = 0.00060"$ for analytical methods.

Since very little can be done to decrease the manufacturing tolerance of 0.0005", it becomes important to reduce the design errors as much as possible. Consequently the design ordinates should be calculated to at least 0.0001". This, of course, cannot be done graphically and analytical design methods are required.

To illustrate this point, the aerodynamic variations in the test section of a Mach 2.0 nozzle have been calculated. It is assumed that the ordinates are given every 1/2 inch and that the total y-error of the graphically designed nozzle is 0.00150" and that of the analytic nozzle is 0.00060". By use of these values and Figure 1.2, the per cent disturbances in the test section of a Mach 2.0 nozzle are tabulated below.

Error In	Graphical Nozzle N=1	N=3	N=5	Analytic Nozzle N=1	N=3	N=5
Static Pressure %	.976	2.928	4.880	.391	1.173	1.955
Force Coefficient %	.762	2.286	3.810	.305	.915	1.525
Mach Number %	.312	.936	1.560	.125	.375	.625

N is the number of reflections of a wave originating at a contour defect. N = 1 corresponds to a nozzle region near the test section, and N = 5 or more to a region near the throat.

It is obvious that in addition to designing a supersonic nozzle by analytical methods, every effort should be made

to improve the manufacturing tolerances, especially near the throat.

4. Review of Analytic Design Methods for Symmetric Nozzles

For the design of symmetric nozzles, several practical and accurate methods are available. In addition to the many graphical and semigraphical procedures based on the method of characteristics, there are the analytical methods due to Foelsch (References 3,4), Friedrichs (References 5,6), Nilson (References 7,8), and Lighthill (Reference 9).

Foelsch uses the concept of radial (source) flow over some downstream portion of the region II (see Figure 1.1) to calculate analytically the patching Mach line and then the contour of the recompression region III. A certain amount of approximation by any suitable method is required, however, to extend these contours through the throat into the subsonic portion.

The other three methods are conceptually the same; Friedrichs treats the axisymmetric nozzle, while Nilson and Lighthill cover the two-dimensional case. Since Lighthill's development is primarily mathematical with emphasis on the transonic region in the hodograph plane, it is less suitable to nozzle contour computations than the other two. Therefore, only the Friedrichs-Nilson concept is reviewed below. Their basic idea is used later to develop the necessary equations for the case of an asymmetrical two-dimensional nozzle.

The continuity and irrotationality equations for com-

pressible, steady flow are written in terms of stream function and velocity potential as independent variables. Together with Bernoulli's equation for an isentropic gas, and a suitably chosen analytic velocity distribution along the axis, a solution is obtained by expanding the dependent variables in powers of the stream function. For a constant value of the stream function, the nozzle contour and flow characteristics are then determined. This solution applies to the supersonic and subsonic regions without any specifications on the shape of the sonic line. The recompression contour is determined by the equations of simple wave flow after the differential equation of the patching Mach line has been integrated numerically.

Although the limits of convergence of this series solution cannot be given explicitly this method is very accurate and useable. Supersonic nozzles built on the basis of this method have performed admirably.

CHAPTER II

PERFECT FLUID THEORY OF ASYMMETRICAL NOZZLE CONTOURS FOR A GIVEN EXIT MACH NUMBER

1. Fundamental Equations in Curvilinear Co-ordinates

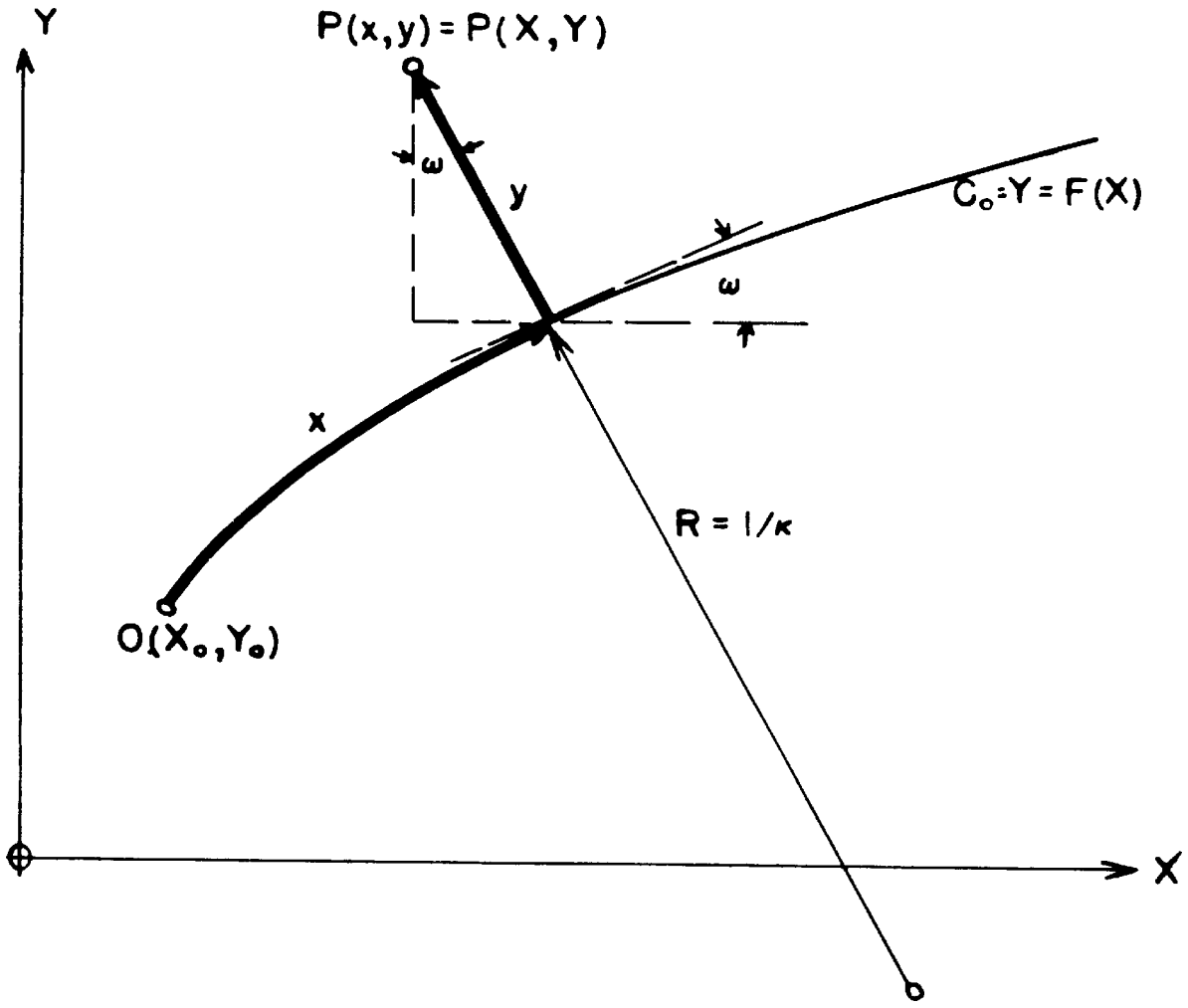
This chapter gives the derivation of the basic equations for steady, irrotational flow of a compressible, isentropic gas through an asymmetric supersonic nozzle. Such a nozzle can be divided into the following regions (see Figure 1.1): subsonic portion - region I; supersonic expansion and reflection region - region II; supersonic simple wave region - region III; test section with uniform supersonic flow - region IV.

Sections 1 through 3 of this chapter apply to the nozzle regions I and II, while sections 4 to 7 deal with the remaining regions III and IV. All steps necessary for the design of a complete nozzle are summarized in section 8.

a) Co-ordinate systems

In view of the curved asymmetric contours the use of curvilinear co-ordinates suggests itself. These co-ordinates may conveniently be chosen along and normal to a reference curve C_o, usually the lower contour. Let (x,y) denote such curvilinear co-ordinates and let (X,Y) stand for the Cartesian base. Then x is measured along the reference curve $C_o = C_o(X,Y)$ and y is measured normal to it. The relations between (x,y) and (X,Y), as well as the curvature κ of the reference curve, can be derived from Figure 2.1 giving

FIGURE 2.1



Curvilinear Co-ordinates

$$\left.\begin{aligned} X &= X_o + \int_o^x \cos\omega\, dx - y \sin\omega \;, \\ Y &= Y_o + \int_o^x \sin\omega\, dx + y \cos\omega \;. \end{aligned}\right\} \qquad (2.1)$$

$$\left.\begin{aligned} \kappa(x) &= \frac{1}{R} = \frac{d\omega}{dx} = \frac{d^2Y/dX^2}{[1+(dY/dX)^2]^{3/2}} \;, \\ \omega &= \int \kappa(x)\,dx = \tan^{-1}(dY/dX) = \tan^{-1} F'(X) \;. \end{aligned}\right\} \qquad (2.2)$$

A flow field in the curvilinear x-y-system can be described by its resultant velocity $q = \sqrt{u^2 + v^2}$ at point P(x,y); in this expression u is the velocity component in x-direction and v is the component in y-direction.

From the geometry of Figure 2.2 it can be seen that a point P(x,y) in the flow field around the reference curve C_o moves an infinitesimal distance to point P[x + (1 + κ y)dx, y+dy] since the distance PP' is equal to

$$dx + y\,d\epsilon = dx + y\frac{dx}{R} = dx + \kappa y\,dx = (1+\kappa y)\,dx \;.$$

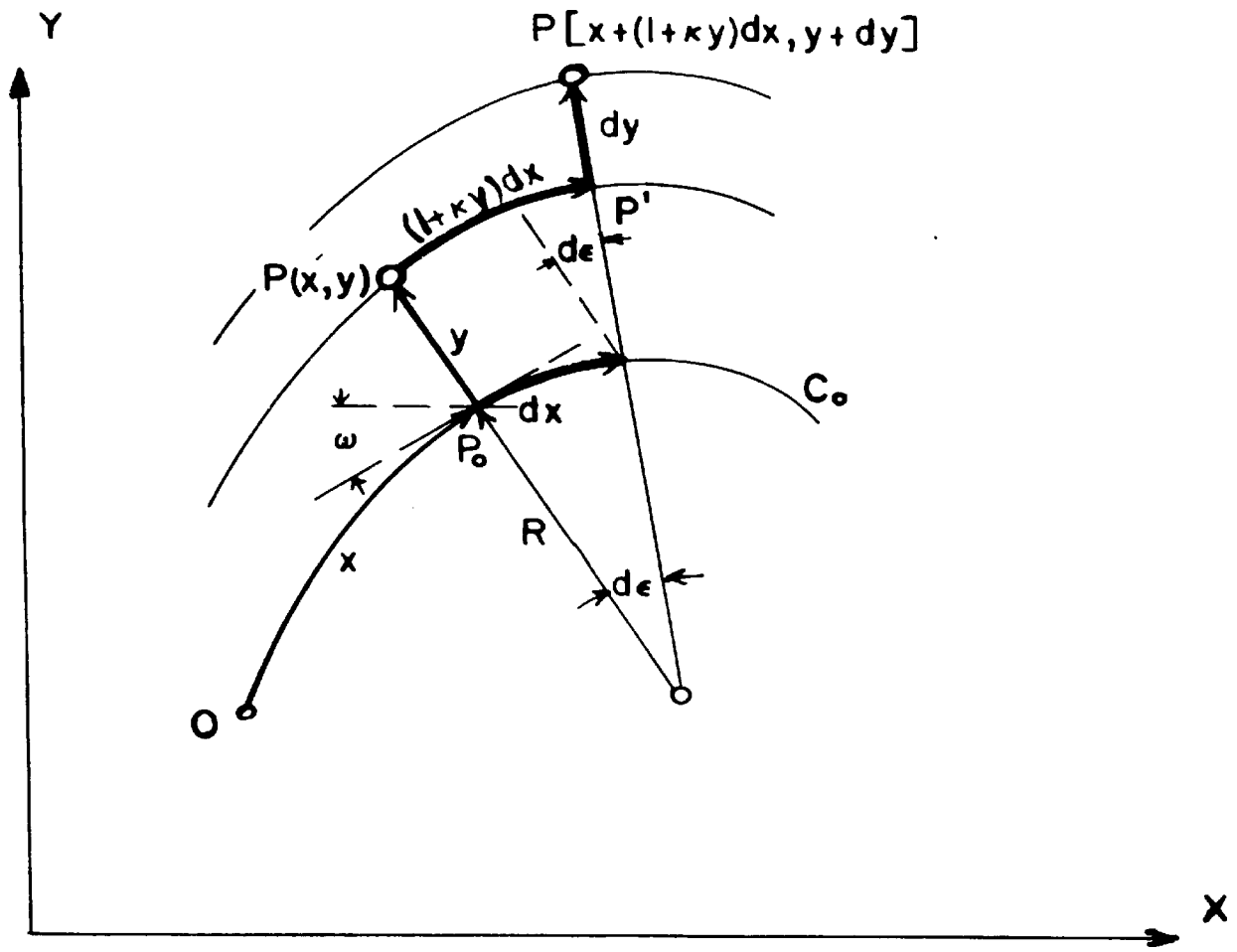
b) Velocity Potential and Stream Function

The continuity equation

$$\mathrm{div}(\rho \vec{q}) = 0 \;, \qquad (2.3)$$

FIGURE 2.2

Differential Geometry in Curvilinear Co-ordinates



and the condition of irrotationality

$$\text{curl } \vec{q} = 0 \quad , \tag{2.4}$$

can be given in terms of the curvilinear co-ordinates (x,y) as follows

$$\frac{\partial(\rho u)}{\partial x} + \frac{\partial}{\partial y}\left[(1+\kappa y)(\rho v)\right] = 0 \quad , \tag{2.5}$$

and

$$\frac{\partial v}{\partial x} - \frac{\partial}{\partial y}\left[(1+\kappa y)u\right] = 0 \quad . \tag{2.6}$$

The derivation of these equations is given in Appendix A. A most general derivation for the case of three dimensional flow is given by Goldstein, Reference 10, page 101.

A stream function ψ (x,y) can be defined which satisfies equation (2.5), i.e.

$$\left.\begin{aligned} \frac{\partial \psi}{\partial y} &= \rho u \quad , \\ \frac{\partial \psi}{\partial x} &= -(1+\kappa y)\rho v \quad . \end{aligned}\right\} \tag{2.7}$$

Similarly, a velocity potential φ (x,y) exists such that

equation (2.6) is true:

$$\left.\begin{aligned} \frac{\partial \varphi}{\partial x} &= (1+\kappa y)u \quad , \\ \frac{\partial \varphi}{\partial y} &= v \quad . \end{aligned}\right\} \qquad (2.8)$$

These equations can easily be verified by substitution into equations (2.5) and (2.6).

c) Transformation of Basic Equations

It is quite common to describe the flow field using the flow direction θ (x,y) and the resultant velocity q(x,y) as dependent variables. These are related to the basic equations through the previously defined functions φ (x,y) and ψ (x,y).

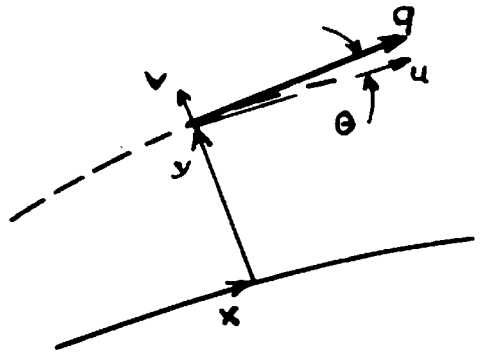


FIGURE 2.3

Velocity And Flow Direction As Field Variables

It was shown by Friedrichs, et. al., in References 5

and 6, and by Lighthill, Reference 9, that it is advantageous to interchange dependent and independent variables. This transformation from $\varphi(x,y)$, $\psi(x,y)$ to $x(\varphi,\psi)$, $y(\varphi,\psi)$ is, of course, subject to the restriction that the Jacobian of the transformation is non-vanishing, i.e.

$$J = \frac{\partial(\varphi,\psi)}{\partial(x,y)} = \rho(1+\kappa y)q^2 \neq 0 . \qquad (2.9)$$

The transformation is therefore valid in the entire flow field of the nozzle since only stagnation points ($q = 0$) and the centers of the curvature ($y = -\frac{1}{\kappa}$) are excluded. Hence, we shall transform our equations using the velocity potential φ and the stream function ψ as independent variables, and x, y, q, and Θ, as dependent variables.

It is straightforward, but lengthy, to transform equations (2.7) and (2.8) from the curvilinear co-ordinates (x,y) to the new curvilinear co-ordinates (φ,ψ) and to replace (u,v) by (q,Θ). It is more convenient to derive these equations directly from the physical definitions of stream function and velocity potential.

Let us consider the orthogonal system of lines (co-ordinates) φ = constant and ψ = constant. Let s be the arc length along a streamline ψ = constant and n the arc length along a potential line φ = constant, which will be normal to s. Then the expressions $\partial y/\partial\varphi$ and $(1+\kappa y)\partial x/\partial\varphi$ are directional derivatives along a stream-

line (φ = constant) and can be written as (Figure 2.4)

$$\frac{(1+\kappa y)\partial x}{\partial \varphi} = \frac{ds}{d\varphi} \cos\Theta \quad ,$$

$$\frac{\partial y}{\partial \varphi} = \frac{ds}{d\varphi} \sin\Theta \quad .$$

The directional derivatives along a potential line (φ = constant) are similarly (Figure 2.4)

$$\frac{(1+\kappa y)\partial x}{\partial \psi} = -\frac{dn}{d\psi} \sin\Theta \quad ,$$

$$\frac{\partial y}{\partial \psi} = \frac{dn}{d\psi} \cos\Theta \quad .$$

By definition of the velocity potential φ,

$$\frac{d\varphi}{ds} = q \quad ;$$

and by definition of the stream function ψ,

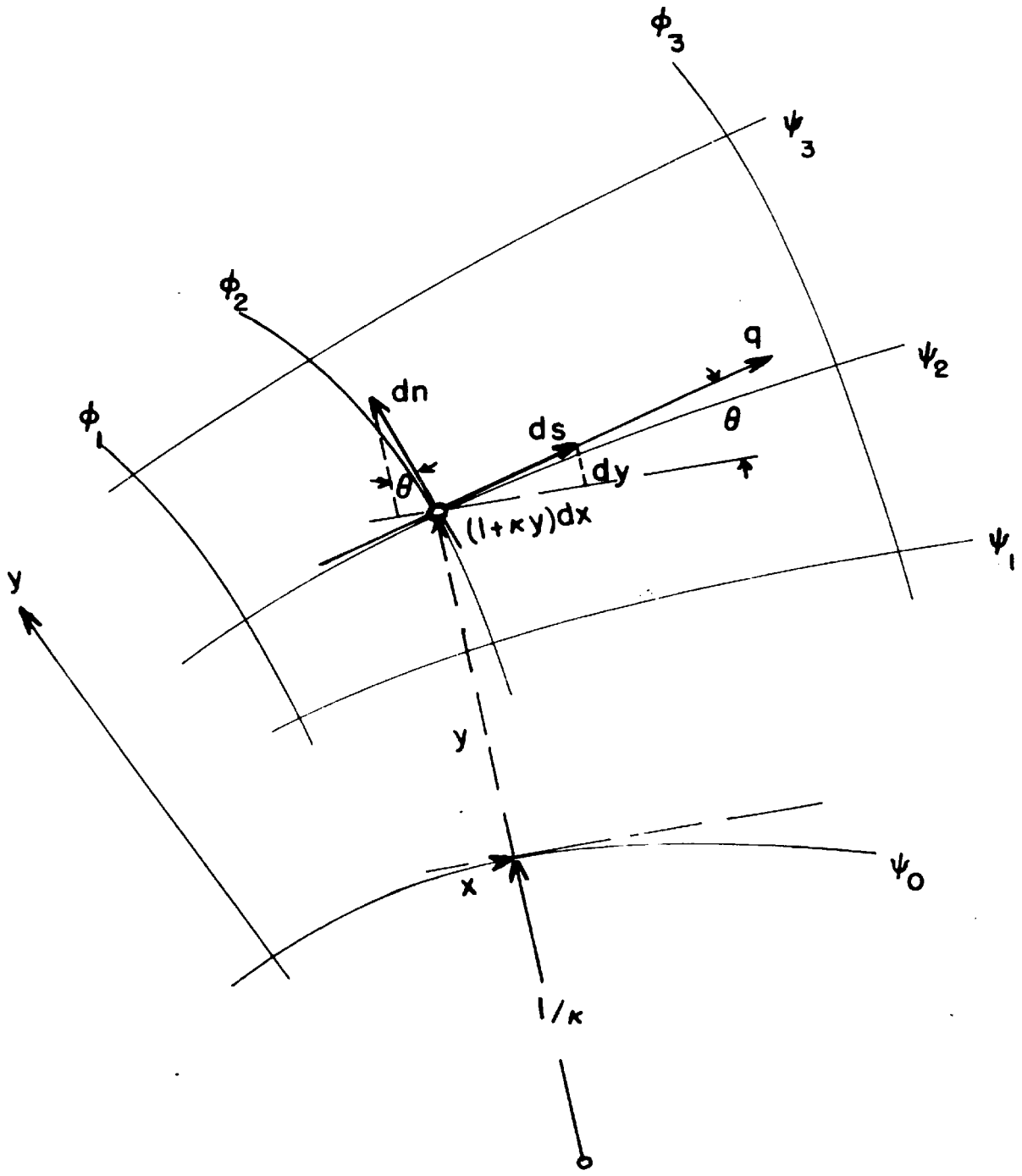
$$\frac{d\psi}{dn} = \rho q \quad .$$

Hence we get the following equations instead of equations (2.7) and (2.8).

$$(1+\kappa y)\frac{\partial x}{\partial \varphi} = \frac{\cos\Theta}{q} \quad , \qquad (2.10)$$

FIGURE 2_4

Streamlines and Potential Lines in Flow Field



$$\frac{\partial y}{\partial \varphi} = \frac{\sin \Theta}{q} , \qquad (2.11)$$

$$(1+\kappa y)\frac{\partial x}{\partial \varphi} = -\frac{\sin \Theta}{\rho q} , \qquad (2.12)$$

$$\frac{\partial y}{\partial \psi} = \frac{\cos \Theta}{\rho q} . \qquad (2.13)$$

For the application to nozzle design it will be convenient to introduce independent variables (ξ , η) having the dimensions of length, in lieu of φ and ψ . This is accomplished by the substitutions

$$\psi = \rho^* q^* \eta , \qquad (2.14)$$

$$\varphi = \int_{\xi_0}^{\xi} q_0(x)\, dx . \qquad (2.15)$$

Here $q_o(x)$ is the known (or assumed) velocity distribution along the reference streamline $\psi_o\,(x,y = 0) = 0$ or $\eta\,(x,y = 0) = 0$; and ρ^* and q^* are the critical density and velocity, respectively, corresponding to sonic flow conditions.

Before carrying out this substitution it is well to define a non-dimensional parameter, h(x,y) which will conveniently occur throughout the subsequent development. This parameter h is proportional to a one-dimensional area ratio and is defined as

$$h = \frac{\rho^* q^*}{\rho\, q} = \frac{A}{A^*} \quad . \qquad (2.16)$$

Substitution of equations (2.14) and (2.16) into equations (2.10) through (2.13) leads to the following four differential equations for x, y, q, Θ, and h(ρ ,q) as functions of ξ and η , and the known parameters κ (x) and $q_o(x)$

$$\frac{\partial x}{\partial \xi} = \frac{\partial x}{\partial \varphi}\frac{d\varphi}{d\xi} = \frac{q_o}{q}\frac{\cos\Theta}{1+\kappa y} \quad , \qquad (2.17)$$

$$\frac{\partial x}{\partial \eta} = -\,h\,\frac{\sin\Theta}{1+\kappa y} \quad , \qquad (2.18)$$

$$\frac{\partial y}{\partial \xi} = \frac{q_o}{q} \sin\Theta \quad , \tag{2.19}$$

$$\frac{\partial y}{\partial \eta} = h \cos\Theta \quad . \tag{2.20}$$

It is possible to eliminate x and y (except for the $1 + \kappa y$) - term) by equating the partial cross-derivatives

$$\frac{\partial}{\partial \eta}\left[\frac{q_o}{q}\,\frac{\cos\Theta}{1+\kappa y}\right] = \frac{\partial}{\partial \xi}\left[-h\,\frac{\sin\Theta}{1+\kappa y}\right] \quad , \tag{2.21}$$

$$\frac{\partial}{\partial \eta}\left[\frac{q_o}{q}\sin\Theta\right] = \frac{\partial}{\partial \xi}\left[h\cos\Theta\right] \quad . \tag{2.22}$$

After differentiating one multiplies equation (2.21) by $(1 + \kappa y)\cos\Theta$ and $-(1 + \kappa y)\sin\Theta$, and equation (2.22)

by $\sin\theta$ and $\cos\theta$, respectively. The respective addition of equations (2.21) and (2.22) leads then to

$$\frac{\partial}{\partial\eta}\left(\frac{q_0}{q}\right) + \frac{q_0}{q}(1+\kappa y)\cos^2\Theta\,\frac{\partial}{\partial\eta}\left(\frac{1}{1+\kappa y}\right) = h\left[(1+\kappa y)\sin\Theta\cos\Theta\,\frac{\partial}{\partial\xi}\left(\frac{1}{1+\kappa y}\right) + \frac{\partial\Theta}{\partial\xi}\right], \tag{2.23}$$

$$\frac{q_0}{q}\left[\frac{\partial\Theta}{\partial\eta} - (1+\kappa y)\sin\Theta\cos\Theta\,\frac{\partial}{\partial\eta}\left(\frac{1}{1+\kappa y}\right)\right] = \frac{\partial h}{\partial\xi} + h(1+\kappa y)\sin^2\Theta\,\frac{\partial}{\partial\xi}\left(\frac{1}{1+\kappa y}\right). \tag{2.24}$$

These two non-linear, first order, partial differential equations are, of course, insufficient to determine the remaining four unknowns q, y, Θ, and h. The additional relations needed are the isentropic equation of state and the Bernoulli equation. These will now be used to obtain a functional relationship between q and h.

d) Bernoulli's Equation and Equation of State

Bernoulli's equation in our notation is

$$\frac{q^2}{2} + \frac{c^2}{\gamma-1} = \frac{\gamma+1}{2(\gamma-1)}\,q^{*2}, \tag{2.25}$$

where $C = \sqrt{\gamma P/\rho}$ is the local speed of sound.

If one eliminates the pressure from the speed of sound by means of the isentropic equation of state

$$P = \rho^{\gamma} \quad , \tag{2.26}$$

one can write Bernoulli's equation in the form

$$C^2 = \frac{\gamma+1}{2} q^{*2} - \frac{\gamma-1}{2} q^2 = q^{*2}\left(\frac{\rho}{\rho^*}\right)^{\gamma-1}; \tag{2.27}$$

or

$$\frac{\rho}{\rho^*} = \left[\frac{\gamma+1}{2} - \frac{\gamma-1}{2}\left(\frac{q}{q^*}\right)^2\right]^{\frac{1}{\gamma-1}}. \tag{2.28}$$

Substitution of (2.28) into equation (2.16) gives the needed relation between q and h,

$$h = \frac{q^*}{q}\left[\frac{\gamma+1}{2} - \frac{\gamma-1}{2}\left(\frac{q}{q^*}\right)^2\right]^{\frac{-1}{\gamma-1}}. \tag{2.29}$$

The distribution of the parameter h along the reference streamline, along which $q_o(x)$ is given, is then also known and given by

$$h_o(x) = \frac{q^*}{q_o}\left[\frac{\gamma+1}{2} - \frac{\gamma-1}{2}\left(\frac{q_o}{q^*}\right)^2\right]^{\frac{-1}{\gamma-1}} . \quad (2.30)$$

From equations (2.29) and (2.30) one gets

$$\frac{h}{h_o} = \left(\frac{q}{q_o}\right)^{-1}\left[\frac{(\gamma+1)-(\gamma-1)\left(\frac{q_o}{q^*}\right)^2\left(\frac{q}{q_o}\right)^2}{(\gamma+1)-(\gamma-1)\left(\frac{q_o}{q^*}\right)^2}\right]^{\frac{-1}{\gamma-1}} . \quad (2.31)$$

It is also desirable to determine the Mach number $M_o(x)$ along the reference streamline in terms of $h_o(x)$ or $q_o(x)$. Divide equation (2.25) by q_o and solve for

$$M_o^2 = \left(\frac{q_o}{c}\right)^2 = \frac{2\left(\frac{q_o}{q^*}\right)^2}{(\gamma+1)-(\gamma-1)\left(\frac{q_o}{q^*}\right)^2} . \quad (2.32)$$

Solving for $\left(\frac{q_o}{q^*}\right)$ and substituting into equation (2.30) gives

$$h_o = \frac{1}{M_o}\left[\frac{2+(\gamma-1)M_o^2}{\gamma+1}\right]^{\frac{\gamma+1}{2(\gamma-1)}} . \quad (2.33)$$

For direct comparison with experimental data the equation for the static pressure will be needed. The ratio of the

pressure $p(\xi,\eta)$ to the pressure $p(\xi, \eta = 0)$ is obtained from equations (2.16), (2.26), and (2.28), and is

$$\frac{p}{p_o} = \left(\frac{\rho}{\rho^*}\frac{q}{q^*}\frac{q^*}{q}\right)^{\gamma}\frac{p^*}{p_o} = \left(\frac{q}{q_o}\frac{h}{h_o}\right)^{-\gamma}, \quad (2.34)$$

where $p_o = p_o(x)$ is the static pressure distribution along the reference streamline.

2. Solution of Differential Equations

Following the example of Friedrichs (References 5,6) and Nilson (References 7,8) a solution of equations (2.18), (2.20), (2.23) and (2.24) is obtained by assuming a power series in η for the dependent variables x, y, q, and Θ and by utilizing the relation between q and h given in (2.29).

Let the reference streamline $\eta = 0$ be the wall of the nozzle along which the velocity distribution q_o and curvature κ are known, and let the origin $x = 0$ be taken at the point where $q_o = q^*$. Then the boundary conditions along the wall $\eta = 0$ can be written:

$$\left.\begin{aligned} \eta &= 0, \\ y &= 0, \\ \Theta &= 0, \\ q &= q_o \end{aligned}\right\} \quad (2.35)$$

Since $(\kappa y)_{y \to 0} = 0$, the substitution of equations (2.35) into equations (2.17) and (2.18) gives

$$\left.\begin{aligned} \left(\frac{\partial x}{\partial \xi}\right)_{\eta=0} &= 1 \,, \\ \left(\frac{\partial x}{\partial \eta}\right)_{\eta=0} &= 0 \,. \end{aligned}\right\} \qquad (2.36)$$

Series solutions for x, y, q, and Θ are written below, incorporating equations (2.35) and (2.36).

$$x = \xi + x_1(\xi)\eta + x_2(\xi)\eta^2 + x_3(\xi)\eta^3 + \cdots \,, \qquad (2.37)$$

$$y = y_1(\xi)\eta + y_2(\xi)\eta^2 + y_3(\xi)\eta^3 + \cdots \,, \qquad (2.38)$$

$$q = q_0\left[1 + q_1(\xi)\eta + q_2(\xi)\eta^2 + q_3(\xi)\eta^3 + \cdots\right] \,, \qquad (2.39)$$

$$\Theta = \Theta_1(\xi)\eta + \Theta_2(\xi)\eta^2 + \Theta_3(\xi)\eta^3 + \cdots \,. \qquad (2.40)$$

The coefficients of powers of η must now be found by substitution into the differential equations (2.18), (2.20), (2.23) and (2.24). These equations also contain the parameter h which can be written in terms of an η - series by means of equations (2.31) and (2.39).

The actual process of determining the coefficients of the η - series is rather time and paper consuming, even if it is carried out to η^3- terms only. The detailed calculations and coefficients are given in Appendix B. For nozzle applications the curvature is small enough so that K^2 and higher order terms can be neglected. After frequent application of the binomial theorem, and equating like powers of η , one can solve for x-, y-, q-, and Θ - coefficients in terms of the known $K(\xi)$, $h_o(\xi)$, and $M_o(\xi)$ and their derivatives with respect to ξ which are denoted by primes. Substitution of these coefficients into equations (2.31), (2.34), and (2.37) through (2.40) gives:

$$x = \xi - \frac{h_o h_o'}{2}\eta^2 + \left\{ \frac{\kappa h_o^2 h_o' M_o^2}{6(M_o^2-1)}\left[(\gamma+3)M_o^2-2\right] + \frac{\kappa' h_o^3 (M_o^2-1)}{6}\right\}\eta^3, \tag{2.41}$$

$$y = h_o\eta - \frac{\kappa h_o^2(M_o^2-1)}{2}\eta^2 + \frac{h_o}{6}\left\{h_o h_o''(M_o^2-1) - h_o'^2\right\}\eta^3, \tag{2.42}$$

$$\begin{aligned}\frac{q}{q_o} = 1 &- \kappa h_o\eta + \frac{h_o h_o''}{2}\eta^2 - \left\{\frac{\kappa h_o h_o'^2}{6(M_o^2-1)^3}\left[\gamma(\gamma+1)M_o^8\right.\right. \\ &\left. - (2\gamma^2-1)M_o^6 - 3\gamma M_o^4 - 3M_o^2 + 1\right] \\ &+ \frac{\kappa h_o^2 h_o''}{6(M_o^2-1)}\left[(\gamma+4)M_o^4 - M_o^2 - 2\right] \\ &\left. + \frac{\kappa' h_o^2 h_o'}{3(M_o^2-1)}(\gamma+1)M_o^4 + \frac{\kappa'' h_o^3}{6}(M_o^2-1)\right\}\eta^3,\end{aligned} \tag{2.43}$$

$$\theta = h_o' \eta - \left\{ \frac{\kappa h_o h_o' (\gamma+1) M_o^4}{2(M_o^2-1)} + \frac{\kappa' h_o^2 (M_o^2-1)}{2} \right\} \eta^2$$

$$+ \left\{ \frac{h_o^2 h_o''' (M_o^2-1)}{6} + \frac{h_o h_o' h_o''}{6} \left[\frac{(\gamma+1) M_o^4}{(M_o^2-1)} - 1 \right] \right.$$

$$\left. + \frac{\kappa \kappa' h_o^3}{2} (M_o^2-1) \right\} \eta^3 , \qquad (2.44)$$

$$\frac{h}{h_o} = 1 - \kappa h_o (M_o^2-1) \eta + \frac{h_o h_o'' (M_o^2-1)}{2} \eta^2$$

$$- \left\{ \frac{\kappa h_o h_o'^2}{6(M_o^2-1)^2} \left[\gamma(\gamma+1) M_o^8 - (2\gamma^2-1) M_o^6 - 3\gamma M_o^4 - 3M_o^2 + 1 \right] \right.$$

$$+ \frac{2\kappa h_o^2 h_o''}{3} \left[(\gamma+1) M_o^4 - M_o^2 + 1 \right]$$

$$\left. + \frac{\kappa' h_o^2 h_o'}{3} (\gamma+1) M_o^4 + \frac{\kappa'' h_o^3}{6} (M_o^2-1)^2 \right\} \eta^3 ,$$

(2.45)

$$\frac{p}{p_o} = 1 + \kappa h_o \gamma M_o^2 \eta - \frac{h_o h_o''}{2} \gamma M_o^2 \eta^2$$

$$+ \gamma M_o^2 \left\{ \frac{\kappa h_o h_o'^2}{6(M_o^2-1)^3} \left[\gamma(\gamma+1)M_o^8 - (2\gamma^2-1)M_o^6 - 3\gamma M_o^4 - 3M_o^2 + 1 \right] \right.$$

$$+ \frac{\kappa h_o^2 h_o''}{6(M_o^2-1)} \left[(\gamma+1) M_o^4 + 5(M_o^2-1) \right]$$

$$\left. + \frac{\kappa' h_o^2 h_o'}{3(M_o^2-1)} (\gamma+1) M_o^4 + \frac{\kappa'' h_o^3}{6} (M_o^2-1) \right\} \eta^3 . \qquad (2.46)$$

The set of equations give, for constant η, the streamlines (x,y), the speed q, the flow direction Θ, the parameter h and hence the Mach number M (through equation (1.41) dropping the subscript $_o$), and the static pressure p. All of these quantities are given in terms of the curvature κ, and the h_o or M_o distribution along the reference streamline $\eta = 0$. The geometry of the flow field is summarized in Figure 2.5.

3. Discussion of Solution

a) Validity of Solution

It should have been shown that the solution given in

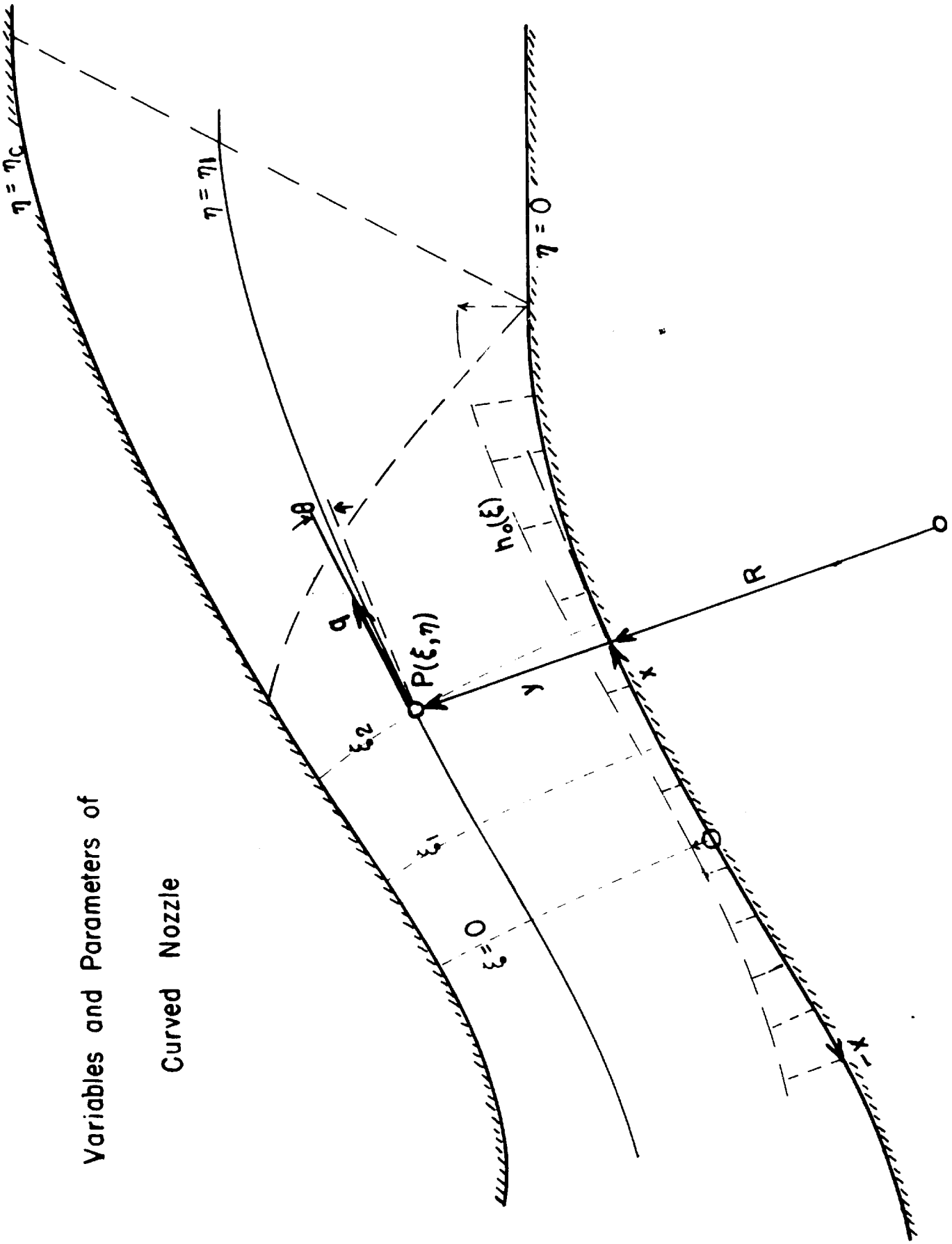


FIGURE 2.5

Variables and Parameters of

Curved Nozzle

the preceeding section is mathematically valid and unique. This is unfortunately not possible and one can only conjecture that under certain conditions a unique solution is likely. Such reasoning has been given by Friedrichs (Reference 5) for the case of an axisymmetric nozzle, and by Lighthill, (Reference 9) for a two-dimensional nozzle. Lighthill, however, uses q^2 and ψ as independent variables instead of φ and ψ used by Friedrichs. Their arguments are as follows:

Instead of solving the boundary value problem for equations (2.7) and (2.8) with prescribed nozzle contours and stagnation conditions, one reverses the problem and determines possible nozzle contours from a velocity distribution q_o, prescribed on one wall. As long as this q_o, or h_o,-distribution is analytic, a unique solution of the differential equations exists, and the series expansion converges in some neighborhood of the wall. One, however, does not know the extent of this neighborhood, except that as long as q, or h, is smooth and analytic along every streamline within the field, the chances of having a valid solution are quite good.

The same argument can be expressed in terms of the streamlines, and one may trust this solution as long as the streamlines are smooth analytic curves. If analytic streamlines are to be pieced together, one must require at least continuity in the curvature of these contours.

For practical applications one must only watch the

value of η_c chosen for the extreme streamline. The results of two-dimensional nozzle calculations by this method (Reference 11) indicate that for design Mach numbers less than 3, and with series which are carried out to η^3 terms, η_c should not exceed .20 and should preferably be around .10. The higher the design Mach number, the smaller should be the maximum value of η, otherwise terms in higher powers of should be retained.

If one calculates a nozzle contour by this method and finds that the η_c-streamline is a smooth and continuous curve and that q, or h, along it are also continuous and smooth, the validity of this solution to the specific problem seems to be assured.

As discussed in section 1-c of this chapter, the non-vanishing of the Jacobian of the transformation from (φ , ψ) to (x,y)-variables is a measure of validity of this transformation. The expression for this Jacobian (Equation 2.9) can now be written in terms of the η-series for ρ, y, and q by substituting equations (2.16), (2.42), (2.43), and (2.45) into equation (2.9).

$$J = \frac{\rho^* q^* q_0}{h_0}\Bigg[1 + \kappa h_0 (M_0^2-1)\eta - \frac{h_0 h_0''}{2}(M_0^2-2)\eta^2$$

$$+\Bigg\{\frac{\kappa h_0 h_0'^2}{6(M_0^2-1)^3}\Big[\gamma(\gamma+1)M_0^{10} - (9\gamma^2+2\gamma-1)M_0^8$$

$$+(9\gamma^2-3\gamma+3)M_0^6 + 6\gamma M_0^4 + 4M_0^2 - 1\Big]$$

$$+\frac{\kappa h_0^2 h_0''}{6(M_0^2-1)}\Big[2(2\gamma-1)M_0^6 - 5(\gamma-2)M_0^4 - 14M_0^2 + 5\Big]$$

$$+\frac{\kappa' h_0^2 h_0'}{3(M_0^2-1)}(\gamma+1)(M_0^2-2)M_0^4 \qquad (2.47)$$

$$+\frac{\kappa'' h_0^3}{6}(M_0^2-2)(M_0^2-1)\Bigg\}\eta^3\Bigg].$$

For specific nozzle problems for which $M_D > 3$ and $\eta_c > .20$ it is suggested that equation (2.47) be calculated for η_c and plotted vs. ξ to detect any strong trend of the Jacobian towards zero. This would appear to be a weaker test for the validity of the solution than the smoothness test of η_c and h, since the Jacobian applies only to the transformation process and not to the series solution of the differential equations of the problem.

b) Special Boundary Conditions

All of the final equations given in the preceeding

sections contain the parameter h_o. It will therefore be useful to write the boundary conditions of the nozzle problem in terms of h_o. From the definition of h (Equation 2.16) it follows that

$$\begin{aligned} h_o &\geqq 1 \ , \\ (h_o)_{\xi=0} &= 1.0 \ , \\ (h_o)_{P_o} &= h_{o_D} \ , \end{aligned} \tag{2.48}$$

The corresponding values of the Mach number are found from equation (2.32) and physical considerations

$$\begin{aligned} (M_o)_{\xi=0} &= 1.0 \ , \\ (M_o')_{\xi=0} &> 0 \ , \\ (M_o)_{P_o} &= M_D \ . \end{aligned} \tag{2.49}$$

Substitution of equations (2.48), and (2.49), into (B-4) of Appendix B, shows that

$$\left(\frac{h_o'}{M_o^2 - 1}\right)_{\xi \to 0} = \text{finite;}$$

hence

$$(h_o')_{\xi \to 0} = 0 \ . \tag{2.50}$$

Furthermore, all terms in the equation for the speed ratio, equation (2.43), must remain finite as $\xi \to 0$. The first two terms of the coefficient of η^3 in this equation require, together with equation (2.50), that

$$\left(\frac{\kappa}{M_o^2-1}\right)_{\xi \to 0} = \text{finite},$$

and

$$\left(\frac{\kappa h_o''}{M_o^2-1}\right)_{\xi \to 0} = \text{finite};$$

i.e.

$$(\kappa)_{\xi \to 0} = 0 . \qquad (2.51)$$

This last result is interesting in that zero curvature at the throat is required without any assumptions having been made regarding the shape of the sonic line. It should be recalled that Görtler (Reference 12) has shown that vanishing wall curvature implies a straight sonic line, and that Sauer (Reference 13) has shown that finite curvature at the throat results in a curved (parabolic) sonic line.

An asymmetric curved nozzle with a curved sonic line is likely to introduce shock waves right at the throat. This condition exists whenever expansion waves hit the sonic line where they are reflected as shock waves. The curvature of the sonic line is rather strong near the expansion wall, and the first few expansion waves downstream from the throat are likely to hit the sonic line. Since the creation of shocks must be avoided in any nozzle design one should avoid a curved sonic line especially in a curved nozzle. A straight sonic line is assured if the wall curvature κ goes to zero at the throat; and it is interesting to note that this desirable condition is a consequence of the general throat boundary condition applied to the η^3 -terms of the q/q_o -equation. The same condition also appears in the series coefficients Θ_2', X_3', and of course q_3 as $\xi \to 0$ (see Appendix B).

4. Equation of Patching Mach Line

The right running Mach line which intersects the starting contour (reference streamline) at a point where the design Mach number is reached is called the patching Mach line. It divides the region of general expansive flow from the simple wave flow. The latter, in turn, is terminated by the design Mach wave further downstream where the desired uniform flow is obtained. In order to calculate the upper contour, which closes the region of simple wave flow, the Mach number and flow direction along the patching Mach line must be known.

The equation of the patching Mach line in (ξ, η) coordinates is determined from the fundamental property that the

angle between flow direction and the tangent to a characteristic (Mach) line at point P is the Mach angle α at that point. From the geometry of Figure 2.6 it is seen that

$$\frac{dy}{(1+\kappa y)dx} = \tan(\theta-\alpha) = -\frac{1+\tan\theta\tan\beta}{\tan\theta+\tan\beta}, \quad (2.52)$$

where

$$\left.\begin{aligned} \alpha &= \sin^{-1}\left(\frac{1}{M}\right), \\ \beta &= \frac{\pi}{2}-\alpha = \tan^{-1}\sqrt{M^2-1}. \end{aligned}\right\} \quad (2.53)$$

Hence

$$(1-\tan\theta\tan\beta)(1+\kappa y)dx+(\tan\theta+\tan\beta)dy = 0. \quad (2.54)$$

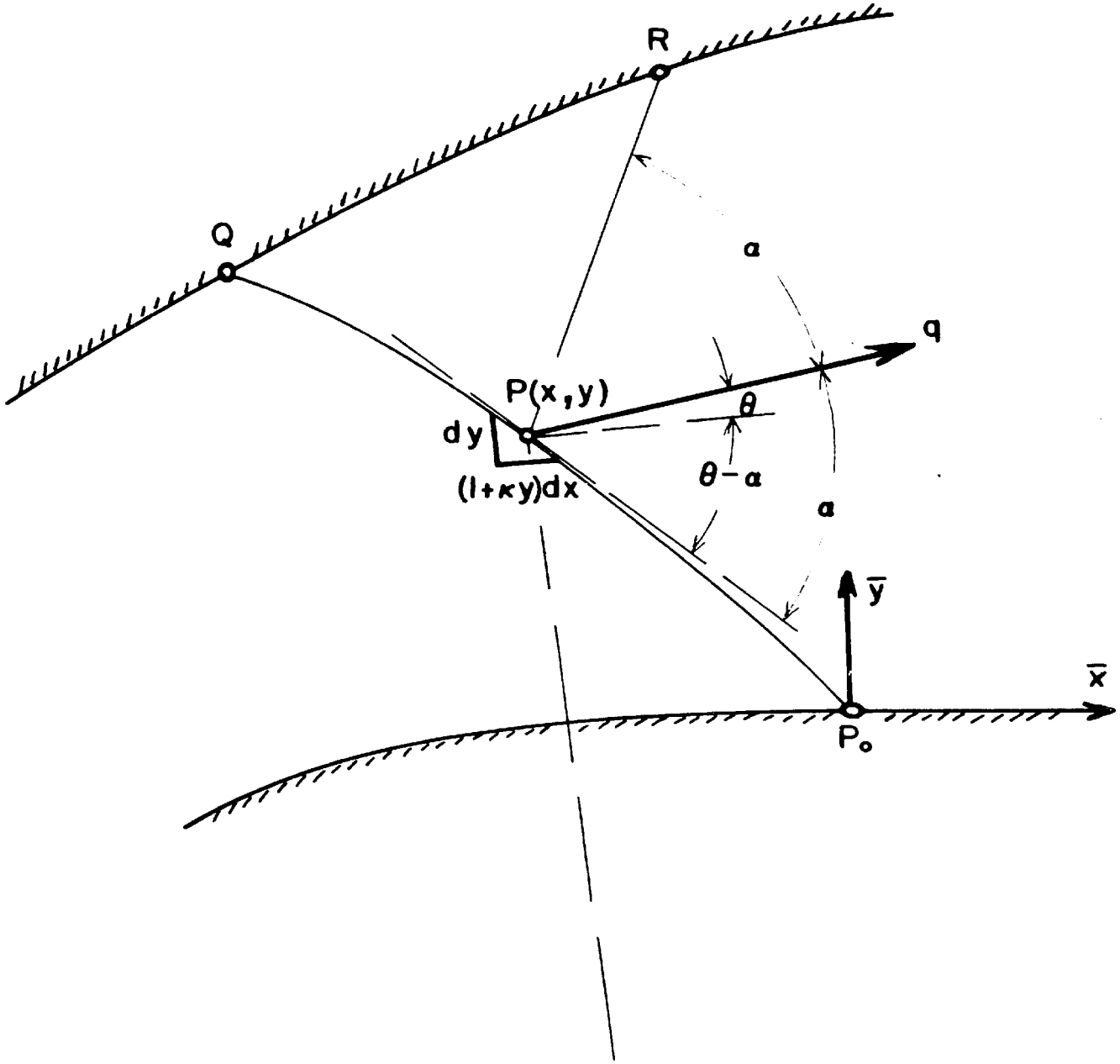
Since

$$dx = \frac{\partial x}{\partial \xi}d\xi + \frac{\partial x}{\partial \eta}d\eta,$$
$$dy = \frac{\partial y}{\partial \xi}d\xi + \frac{\partial y}{\partial \eta}d\eta,$$

one can express equation (2.54) in terms of the η-series. The details of these calculations are given in Appendix C. The final result is the following partial differential equa-

FIGURE 2.6

Patching Mach Line



tion for the patching Mach line

$$\frac{d\eta}{d\xi} = \frac{-1}{h_o\sqrt{M_o^2-1}}\Bigg[1 + \frac{\kappa h_o}{2(M_o^2-1)}(\gamma+1)M_o^4\,\eta$$

$$- \frac{h_o h_o''}{4(M_o^2-1)}(\gamma+1)M_o^4\,\eta^2$$

$$+ (\gamma+1)M_o^4\Bigg\{\frac{\kappa h_o h_o'^2}{12(M_o^2-1)^4}\left[8(\gamma+1)M_o^8 - (2\gamma^2-1)M_o^6\right.$$

$$\left. - 3\gamma M_o^4 - 3M_o^2 + 1\right] \qquad (2.55)$$

$$+ \frac{\kappa h_o^2 h_o''}{24(M_o^2-1)^2}\left[(5\gamma-1)M_o^4 - 4(3\gamma-4)M_o^2 - 22\right]$$

$$+ \frac{\kappa' h_o^2 h_o'}{6(M_o^2-1)^2}\left(\gamma M_o^4 + 2M_o^2 - 1\right)$$

$$+ \frac{\kappa'' h_o^3}{12}\Bigg\}\eta^3\Bigg].$$

Before discussing the solution of the differential equation for the patching Mach line it is worth while to study this equation in the neighborhood of point P_o (Figure 2.6), the initial point of the patching Mach line. A relation is obtained between Mach number distribution M_o along the lower contour and the wall curvature κ which is important for the selection of the function which expresses $M_o = M_o(\xi)$, and $h_o = h_o(\xi)$.

5. Initial Mach Number Distribution and Wall Curvature at the Patching Mach Line

At the point P_o, where the initial Mach number reaches its design value, the curvilinear co-ordinates x and y can be replaced by Cartesian co-ordinates $\bar{x}$ and $\bar{y}$ (Figure 2.6). The radius of curvature of a streamline $\bar{y} = f(\bar{x})$ can be written as

$$\frac{d^2\bar{y}/d\bar{x}^2}{\left[1 + (d\bar{y}/d\bar{x})^2\right]^{3/2}}$$

But at, or near, point P_o the Cartesian co-ordinates can be written as $\bar{x} = \xi - \xi_o$ and $\bar{y} = \eta$. The differential expression for the curvature at point P_o is therefore

$$K_{P_o} = \lim_{\eta \to o} \frac{d^2\eta/d\xi^2}{\left[1 + (d\eta/d\xi)^2\right]^{3/2}} \quad . \qquad (2.56)$$

From equation (2.55) and (B-4) one obtains the following equations

$$(d\eta/d\xi)_{\eta=o} = -h_o^{-1}(M_o^2 - 1)^{-\frac{1}{2}} \quad ,$$

$$\left(d\eta/d\xi\right)^2_{\eta=0} = h_o^{-2}\left(M_o^2-1\right)^{-1} ,$$

$$\left(d^2\eta/d\xi^2\right)_{\eta=0} = h_o' \frac{(\gamma+1)M_o^4 - 2(M_o^2-1)}{2h_o^2(M_o^2-1)^{5/2}} .$$

Substitution of these terms into the curvature equation (2.56) gives

$$K_{P_o} = h_o h_o' \frac{(\gamma+1)M_o^4 - 2(M_o^2-1)}{2\left\{1 + h_o^2(M_o^2-1)\right\}^{3/2}} . \qquad (2.57)$$

Since the wall curvature downstream of P_o is zero and smoothly approaches zero from upstream one has $K_{P_o} = 0$. Thus, equation (2.57) requires that

$$h_{o_{P_o}}' = 0 ,$$

since all other terms are finite at P_o. Therefore, one gets from equation B-4,

$$M_{o_{P_o}}' = 0 . \qquad (2.58)$$

This equation states that the Mach number distribution M_o, initially assumed along the lower contour, must have a con-

tinuous gradient which goes to zero at the patching Mach line, i.e. $(dM/dx)_{P_o}$ or $(dM/d\xi)_{P_o} = 0$. The same statement, of course, applies to the distribution of the parameter h_o, and becomes an important boundary condition for the $h_o = h_o(\xi)$ distribution.

The fact that the Mach number gradient at P_o vanishes assures also continuity of curvature of the opposite contour at the patching Mach line (Point Q in Figures 2.6 and 2.7) and at the test section juncture (Point S in Figure 2.7) (provided of course that $d\eta/d\xi$ is continuous). This was shown by Frost (Reference 14), and Evvard and Marcus (Reference 15), and is one of the desirable and outstanding features of an asymmetric nozzle.

6. Calculation of Patching Mach Line

In order to locate the patching Mach line geometrically and to get the values of Mach number and flow direction along it, one must integrate equation (2.55).

Any method of numerical integration will suffice and only a brief discussion will be given here. It is stressed, however, that this integration should be carried out accurately since the accuracy of locating the recompression contour will depend on an accurate knowledge of the patching Mach line.

The Runge-Kutta method of integration is considered most suitable for this purpose. Frost (Reference 11) calculated a patching Mach line for a two-dimensional symmetric nozzle by Runge-Kutta and by characteristics and found vir-

tually no error. The series approximation, also given below, however, showed noticeable deviations from the Runge-Kutta patching Mach line even for a design value of $\eta_c = .10$.

a) Runge-Kutta Method

Equation (2.55) for the patching Mach line can be written in the form

$$d\eta = [A_0(\xi) + A_1(\xi)\eta + A_2(\xi)\eta^2 + A_3(\xi)\eta^3]d\xi = F(\xi,\eta)d\xi, \quad (2.59)$$

where

$$A_0 = -h_0^{-1}(M_0^2-1)^{-\frac{1}{2}},$$

$$A_1 = -\frac{\kappa(\gamma+1)M_0^4}{2(M_0^2-1)^{3/2}},$$

$$A_2 = \frac{h_0''(\gamma+1)M_0^4}{4(M_0^2-1)^{3/2}},$$

$$A_3 = -\frac{(\gamma+1)M_o^4}{6(M_o^2-1)^{1/2}}\left\{\frac{K h_o'^2}{2(M_o^2-1)^4}\left[\gamma(\gamma+1)M_o^8-(2\gamma^2-1)M_o^6-3\gamma M_o^4-3M_o^2+1\right]\right.$$

$$+\frac{K h_o h_o''}{4(M_o^2-1)^3}\left[(5\gamma-1)M_o^4-4(3\gamma-4)M_o^2-22\right]$$

$$+\frac{K' h_o h_o'}{(M_o^2-1)^2}\left[\gamma M_o^4+2M_o^2-1\right]$$

$$\left.+\frac{K'' h_o^3}{2}\right\} .$$

The first step in the Runge-Kutta integration starts at the known point P_o (ξ_o, $\eta_o = 0$) with a suitably chosen ξ - interval $\Delta\xi$, and is determined from

$$\Delta\eta = \frac{1}{6}(K_1 + 2K_2 + 2K_3 + K_4) \; , \qquad (2.60)$$

where

$$K_1 = F(\xi_o, \eta_o)\,\Delta\xi \; ,$$

$$K_2 = F\left(\xi_o + \frac{\Delta\xi}{2}, \eta_o + \frac{K_1}{2}\right)\Delta\xi \; ,$$

$$K_3 = F(\xi_0 + \frac{\Delta\xi}{2}, \eta_0 + \frac{K_2}{2})\Delta\xi \quad ,$$

$$K_4 = F(\xi_0 + \Delta\xi, \eta_0 + K_3)\Delta\xi \quad .$$

The first point on the patching Mach line, $P_1(\xi_1, \eta_1)$, is then known, since

$$\xi_1 = \xi_0 + \Delta\xi \quad ,$$

$$\eta_1 = \eta_0 + \Delta\eta \quad .$$

The same equations apply to successive intervals until $\eta = \eta_c$ is reached.

b) Series Approximation

For very small η, say for less than .10, a fair approximation for the patching Mach line is obtained by expanding ξ into an η-power series about point P_0

$$\xi = a_0 + a_1\eta + a_2\eta^2 + a_3\eta^3 \quad . \qquad (2.61)$$

Differentiation of equation (2.61) and collection of terms leads to

$$\frac{d\eta}{d\xi} = \frac{1}{a_1} - \left\{\left(\frac{a_1'}{a_1}\right) + 2\left(\frac{a_2}{a_1^2}\right)\right\}\eta$$

$$+ \left\{4\left(\frac{a_2^2}{a_1^3}\right) - 3\left(\frac{a_3}{a_1^2}\right) - \left(\frac{a_2'}{a_1}\right) + 2\left(\frac{a_1'}{a_1}\right)\left(\frac{a_2}{a_1}\right)\right\}\eta^2 . \quad (2.62)$$

The a-coefficients are determined by equating equations (2.62) and (2.55). The results are

$$a_0 = (\xi)_{P_0} = \xi_D \quad ,$$

$$a_1 = h_{o_D}\left(M_D^2 - 1\right)^{1/2} \quad ,$$

$$a_2 = -\frac{h_{o_D} h_{o_D}' \left\{(\gamma+1)M_D^4 - 2(M_D^2 - 1)\right\}}{4(M_D^2 - 1)}$$

$$+ \frac{K h_{o_D}^2 (\gamma+1) M_D^4}{4(M_D^2 - 1)^{1/2}} \quad ,$$

$$a_3 = -\frac{h_{o_D} h_{o_D}'^2}{12(M_D^2-1)^{5/2}}\left[(\gamma+1)M_D^4 - (M_D^2 - 1)\right]$$

$$+ \frac{K h_{o_D}^2 h_{o_D}' (\gamma+1) M_D^4}{24(M_D^2-1)}\left[(5\gamma+3)M_D^4 - 2(2\gamma+1)M_D^2 - 4\right]$$

$$+ \frac{K' h_{o_D}^3 (\gamma+1) M_D^4}{12(M_D^2-1)} \quad . \quad (2.63)$$

Once the coefficients a_0, a_1, a_2, and a_3 have been determined, the parameter ξ for the patching Mach line can be calculated for any value of η from equation (2.61).

7. Calculation of Simple Wave Region

Once the patching Mach line m_o is calculated in terms of (ξ , η) and (x,y); the flow inclination and Mach number along it can be found. These quantities are sufficient to determine the nozzle recompression contour for the simple wave flow region, which turns the flow from patching Mach line m_o into the desired uniform test section flow starting at the design Mach wave m_1.

From Figure 2.7 and the continuity equation expressed in stream function terms one gets

$$\psi_Q - \psi = \psi_R - \psi = \rho c l \quad .$$

The latter expression follows from

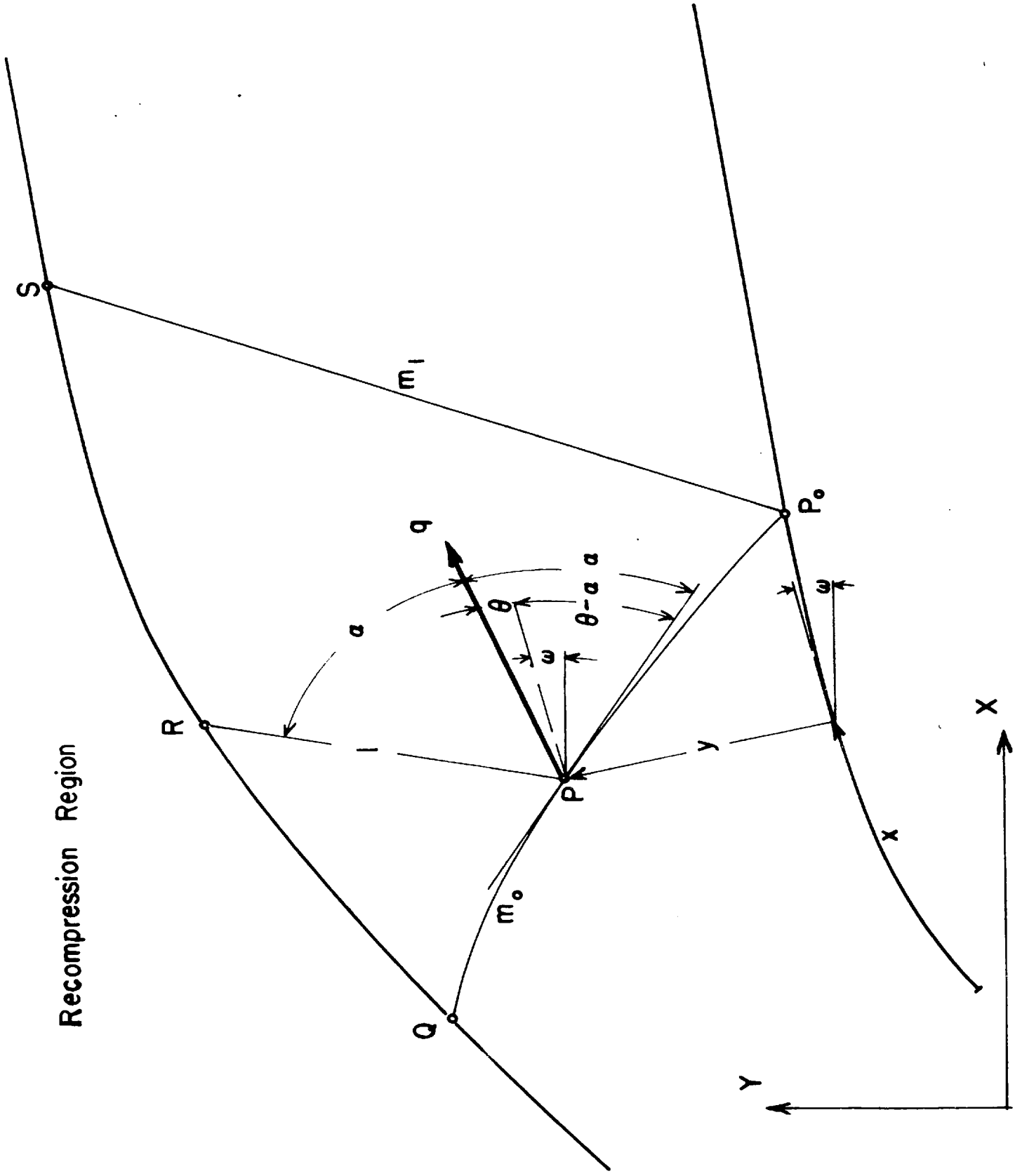
$$(d\psi/ds)_{PR} = \rho c \quad ,$$

where c is the speed of sound at P, in a direction, by definition, normal to the characteristic line PR.

The length of the characteristic line is

$$l = \frac{\psi_Q - \psi}{\rho c} = \frac{\rho^* q^*}{\rho c}(\eta_Q - \eta) = (hM)_P(\eta_Q - \eta) \quad . \quad (2.64)$$

FIGURE 2.7


Recompression Region
S
m_1
P_o
q
θ
$\theta-\alpha$ a
α
ω
R
l
y
P
X
x
m_o
Q
Y

Since $h = \frac{A}{A^*}$ is tabulated in any supersonic isentropic table (Reference 17) it can be read if either M, M*, $\frac{p}{H}$ or any other property of point P is known.

The length l of the characteristic from P determines point R on the nozzle contour, i.e.

$$R = R\left[X + l\cos(\alpha+\theta+\omega), Y + l\sin(\alpha+\theta+\omega)\right] \quad , \qquad (2.65)$$

where α is the Mach angle at P.

In this manner as many points as desired may be calculated for the recompression contour between Q and S.

8. Outline of Complete Nozzle Contour Calculations

A nozzle design problem usually starts from a given design Mach number M_D, and a specified test section height t. In view of the analysis of Chapter I, Section 3, it is suggested that all numerical calculations be carried out to at least the 4th decimal place or 1/10,000 of unity. The major steps in a complete nozzle contour calculation are enumerated below.

1) Determine an analytic expression for the initial lower contour C_o, i.e. Y = F (X). The curvature distribution K (x) can then be calculated from equations (2.1) and (2.2).

2) Select suitable values for ξ_D and η_C. The former, being the ξ -value at the beginning of the test rhombus, can be chosen to make the numerical calculations of the h_o-function as simple as possible. In most cases a ξ_D of unity is very

convenient. This selection will also fix the scale factor for the x-co-ordinates.

Choose a proper value of η_C for the upper contour. This will depend on the value of M_D, the number of η-power terms to be used, and the degree of accuracy desired. As an initial guide use $\eta_C \leqq .20$ for $M_D \leqq 2.0$ and $\eta_C \leqq .10$ for $M_D \geqq 3.0$. (cf. discussion in 3-a). This choice will fix the scale factor for the y-co-ordinate.

3) Assume an analytic expression for the h_o-distribution along the lower contour. For the supersonic region a trigonometric function of the form

$$h_o(\xi)_{M>1} = a + b \sin \pi\left(\frac{\xi + c}{d}\right) \qquad (2.66)$$

is recommended. The constants are determined by the boundary conditions of the particular nozzle (Equations 2.48, 2.50, and 2.58). The subsonic distribution can be expressed as

$$h_o(\xi)_{M<1} = a + b \sin \pi\left(\frac{\xi + c}{d}\right) + e\xi^3 + \cdots, \qquad (2.67)$$

where the odd power terms in ξ assure the more rapid opening of the subsonic channel towards the nozzle entrance. Such a distribution is useable between the throat and the subsonic point of inflection. The region between the nozzle entrance and subsonic point of inflection requires either a third h_o

distribution or an analytic fairing of the final contours. The several h_o functions must of course have continuous first and second derivatives throughout and especially where two join each other.

In addition to the functions $h_o(\xi)$, $h_o'(\xi)$, $h_o''(\xi)$, and $h_o'''(\xi)$ one needs the expressions $\kappa(\xi)$ and $M_o(\xi)$. The curvature function $\kappa(\xi)$ is easily obtained from the $\kappa(x)$ of step 1. Some fairing may be needed near the throat and the patching Mach line where $\kappa(\xi)$ goes to zero rapidly.

The $M_o(\xi)$ distribution cannot be given explicitly but must be calculated for each $h_o(\xi)$-value from either equation (2.33) or read from an accurate isentropic table, such as Reference 17, corresponding to the value of $h_o(\xi) = A/A^*$. Such an isentropic table will at the same time give the ratio of static to stagnation pressure p/H along the lower contour.

4) Calculate x(Equation 2.41), y(Equation 2.42), θ (Equation 2.44), p/p_o (Equation 2.46), and, possibly, q/q_o (Equation 2.43), h/h_o (Equation 2.45), and J (Equation 2.47), for η_C and for as many ξ-stations as are desired between the largest negative ξ-value and about (.6 to .7) ξ_D. The curvilinear co-ordinates (x,y) together with the proper scale factors and equation (2.1) will give the Cartesian co-ordinates for the upper contour. Running plots of all coefficients as well as η-terms vs. ξ will serve to detect numerical errors.

5) Calculate the patching Mach line over the range

$.5 \leq \xi_j \leq \xi_{j,D}$ and $0 \leq \eta \leq \eta_C$ by the Runge-Kutta method (Equation 2.59). Only if $\eta_C < .10$ will the series approximation (Equation 2.61) by useable. After the patching Mach line is determined in terms of ξ and η, the corresponding x, y, Θ, and p/p_o (or h/h_o) values can be calculated from equations (2.41), (2.42), (2.44), and (2.46) (or (2.45)). Equation (2.1) together with these x and y co-ordinates gives the patching Mach line in Cartesian co-ordinates. The Mach angle α is needed also and is read from an isentropic table for the values of p/H or h along the patching Mach line. The upper contour of the simple wave (or recompression) region can now be calculated from equations (2.64) and (2.65).

6) This completes the nozzle contour calculations. For immediate comparison with future experimental data it is advisable to calculate p/H along each nozzle contour.

CHAPTER III

NOZZLE CONTOUR CALCULATIONS FOR AN EXIT MACH NUMBER OF 2.37

1. Introduction

The method developed in Chapter II is now used to calculate a supersonic asymmetric nozzle for a 4 inch high test section and a design Mach number of 2.37. For comparison a very similar nozzle, designed by the method of characteristics, was available (Reference 2). Because of the graphical design procedure of the comparison nozzle it was not possible to express the curvature of the lower (reference) contour, nor the M_o- and h_o-distribution along it, in an analytic form. The analytic functions used are a fair but not exact approximation of their comparison functions. The calculations are carried out for the entire supersonic region and a portion of the high subsonic region.

2. Basic Data

a) h_o-Function

Supersonic Region: For the supersonic region a trigonometric representation for $h_o(\xi)$ was chosen in such a manner that $h_o' = 0$ where the design Mach number is first reached. This assures zero Mach number gradient and also continuity of wall curvatures as discussed in Chapter II, Part 5. It is usually convenient to choose $\xi = 1.0$ at the design value of h_o. The h_o-function of the form (2.66) becomes in

this case

$$h_o = 1.669 + .669 \sin \pi (\zeta - .5).$$

This expression satisfies the boundary conditions

$h_o = 1.0$ at $\zeta = 0$ (throat),

$h_o = 2.338$ at $\zeta = 1.0$ ($M_{design} = 2.37$),

$h_o' = 0$ at $\zeta = 0$, and $\zeta = 1.0$.

Figure 3.1 shows this h_o-function plotted vs. ζ as well as the non-analytic h_o distribution of the comparison nozzle (dotted line). The first derivative h_o' of the analytic distribution is also shown in Figure 3.1, while Figure 3.2 gives the second and third derivatives of h_o.

The Mach number along the lower contour, corresponding to the analytic h_o-function, is plotted in Figure 3.3 as well as M_o of the comparison nozzle (dotted line).

Subsonic Region: The subsonic region is generally shorter than the supersonic one and the subsonic nozzle entrance is larger than the test section. Thus a different h_o distribution is needed to achieve this. The subsonic h_o-function must also be continuous at least in its derivatives h_o' and h_o''. At the throat the comparison nozzle has a section of nearly constant height, about one throat length ($\zeta = .10$) long, to favor the development of a straight sonic line in accordance with Görtler's analysis (Reference 12). This section is faired in between the subsonic and supersonic h_o-distributions used.

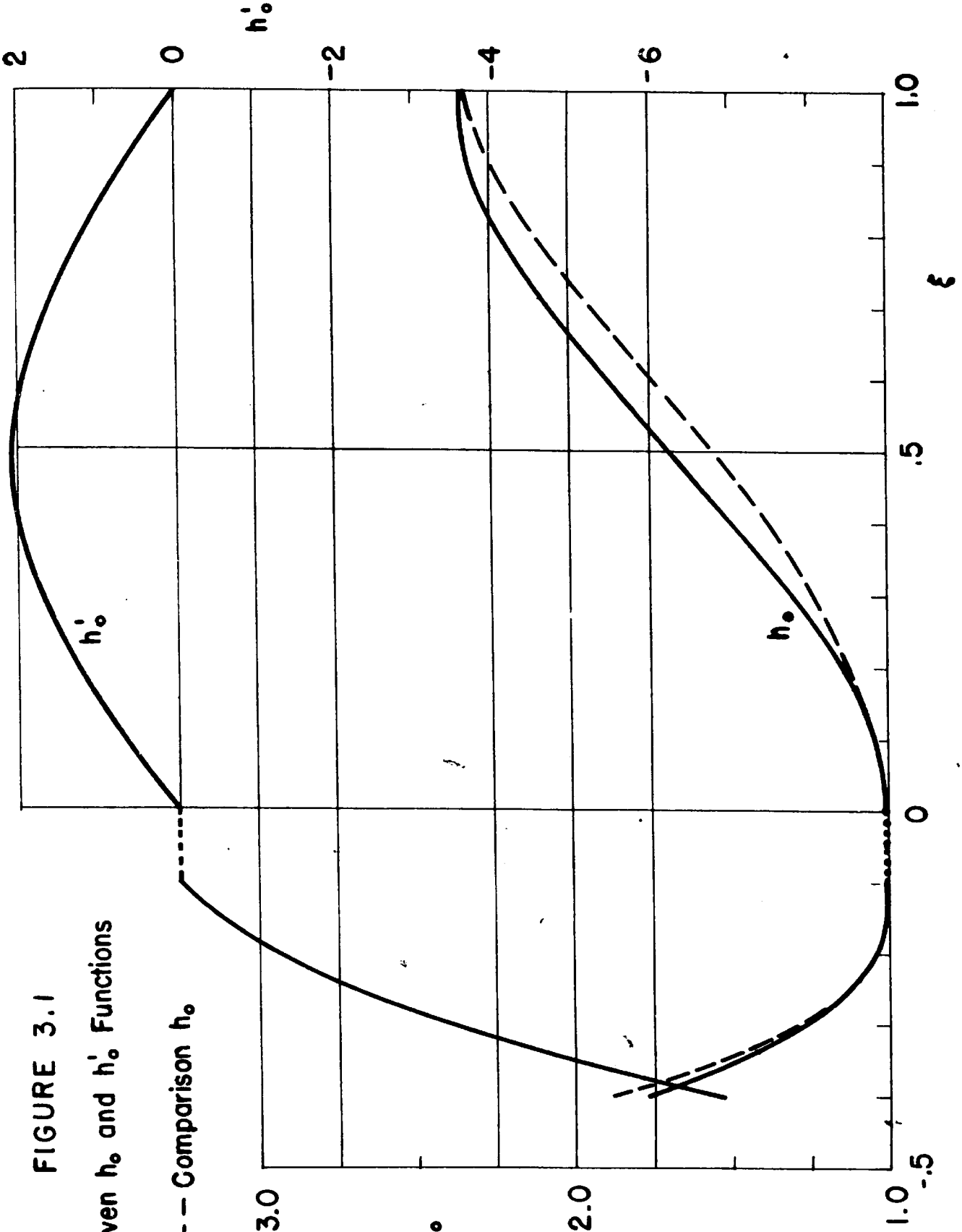
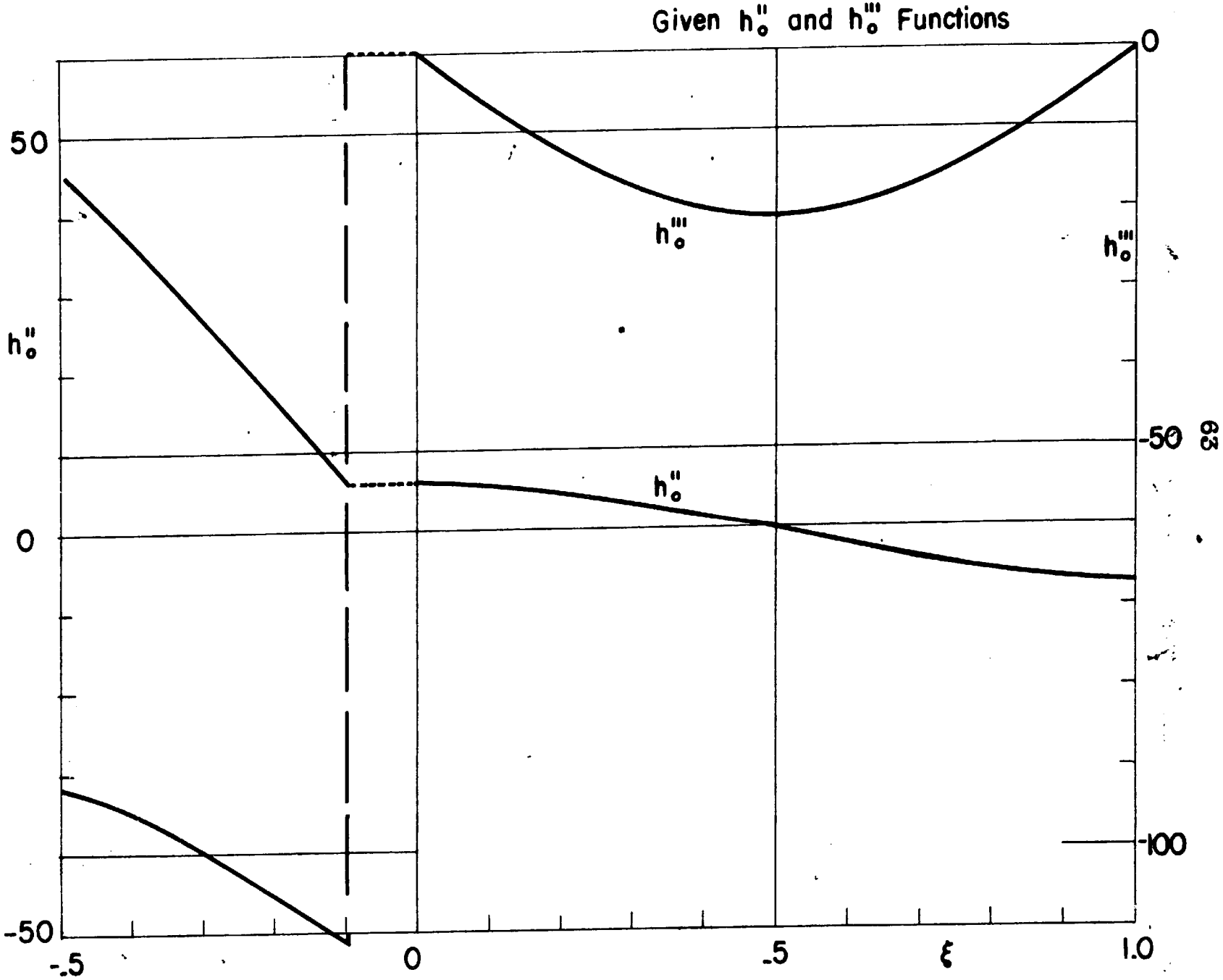


FIGURE 3.1
Given h_0 and h_0' Functions
----- Comparison h_0

FIGURE 3.2



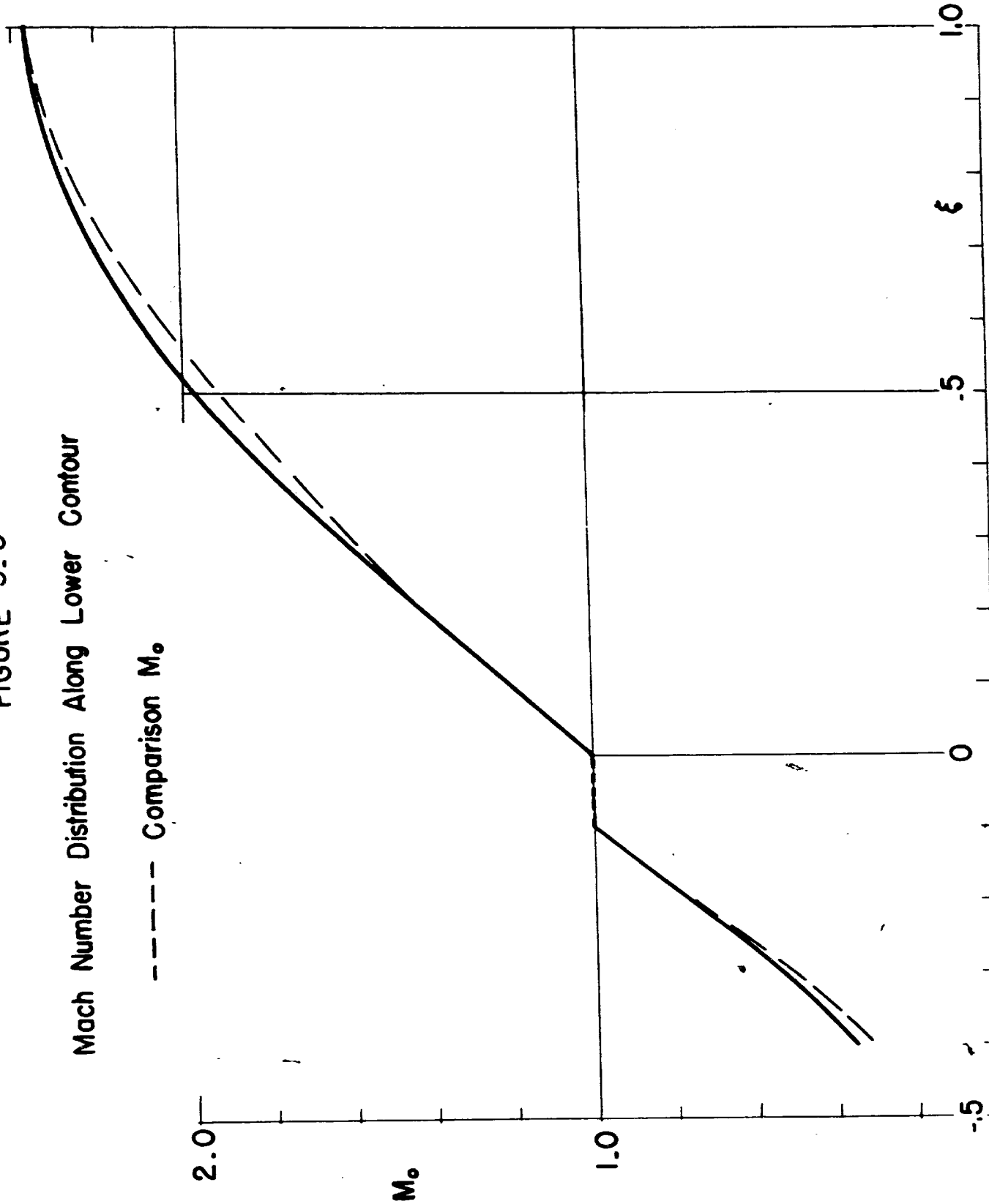


FIGURE 3.3

Mach Number Distribution Along Lower Contour

By use of equation (2.67) the subsonic h_o distribution becomes

$$h_o = 1.669 + .669 \sin \pi(\xi - .4) - 18.65 (\xi + .1)^3,$$

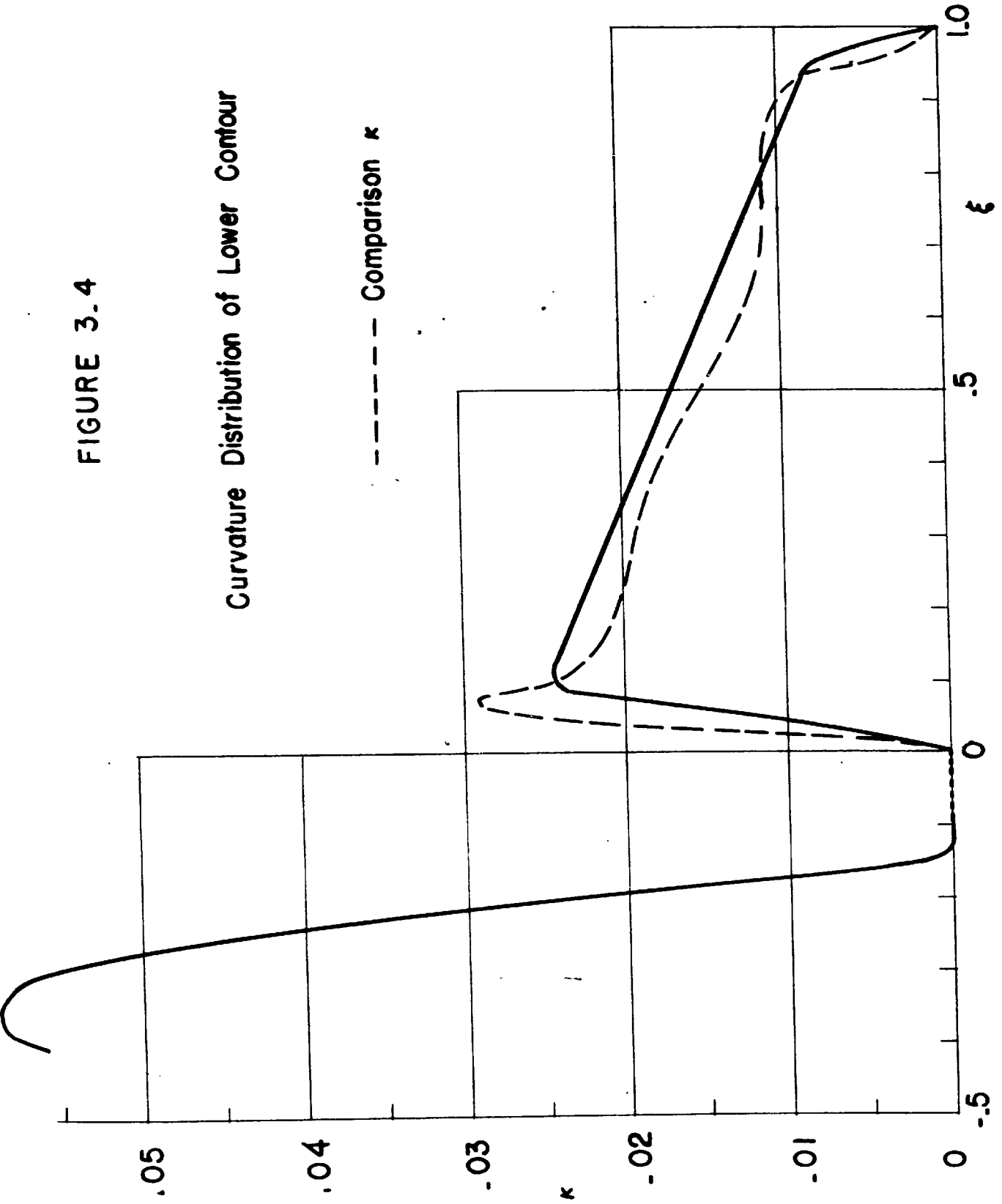
and is valid between $\xi = -.1$ and $-.4$. This function and its derivatives as well as the corresponding M_o values are also shown in Figures 3.1, 3.2, and 3.3.

The subsonic h_o-distribution extends upstream to about the point of inflection in the subsonic contour. From here to the actual nozzle entrance a third h_o distribution is needed such that it and its first and second derivatives are continuous at $\xi = -.4$. The h_o value at the entrance depends on the entrance height and the h_o' value is zero to assure continuous transition. In this region the Mach number is usually so low that a variation of h_o will not affect the flow and the contour too much. It is therefore suggested that the fairing between the subsonic entrance and its point of inflection be done by an analytic equation for the contour itself. A second or third power function or even a trigonometric expression for $y = f(-x)$ will be satisfactory. The details of this last fairing for the determination of a subsonic entrance section have not been carried out since they are straightforward and depend greatly on the exact shape of the entrance geometry.

b) Curvature Distribution

The curvature K of the lower contour is shown in Figure 3.4. Since the lower contour of the comparison nozzle

FIGURE 3.4


Curvature Distribution of Lower Contour
---------- Comparison κ
.05
.04
.03
.02
.01
0
κ
-.5
0
.5
1.0
ξ

was taken as reference contour, its curvature was essentially used. In the supersonic region a straight line was employed to approximate the actual curvature (shown in a dotted line). This line was faired to zero at the throat and the test section.

The results of the subsequent calculations showed that the κ -terms are all very small and that it would have been sufficient to use a constant value of κ throughout.

c) Scale Factors

The η -value for the upper contour was chosen as $\eta_c = .10$ and thus the scale factors for the x and y coordinates in $\xi - \eta$ units are fixed. With a design Mach number of 2.37 and a test section height of 4 inches the throat height becomes 4/2.338 = 1.711". Hence all y-values calculated with $\eta = .10$ must be multiplied by 1.711/ .10 = 17.11" since at the throat $\xi = 0$ and y (in inches) = scale factor (η) (Equation 2.42). The same scale factor applies to the x-values calculated in $\xi - \eta$ units. This follows from the fact that from continuity considerations (y/η) is a fixed ratio and $(x/\xi) = 1/h_d(y/\eta)$ at the design Mach wave. Hence $(x/\xi) = 4/.10 \times 2.338 = 17.11"$ must be the x-scale factor since $\xi = 1.0$ at this point. The scale factor for x can of course be checked or calculated from the actual length (curvilinear) of the reference contour between the throat ($\xi = 0$) and the exit ($\xi = \xi_D$) and the numerical value of ξ_D chosen at this point.

3. Nozzle Contours

a) Subsonic and Supersonic Regions up to the Patching Mach Line

With the basic data given above, values of x, y, p/p_o, q/q_o, and Θ were calculated from equations (2.41), (2.42), (2.46), (2.43) and (2.44), respectively, and are plotted in Figures (3.5) to (3.9). These Figures also show the individual curves for the η-, η^2-, and η^3- terms. One can therefore determine if the η^3-terms could be neglected which are rather massive in many equations. It appears that the η^3-term is important only in the Θ-equation (Figure 3.9) and could well be dropped in the other equations.

It is noted that the η^3-term of y becomes important between ξ = .60 and 1.0 (Figure 3.6). In this region, however, y is used only to calculate the patching Mach line with η-values between 0 (at ξ = 1.0) and .10 (at ξ = .60). Thus the η^3-term of y for the patching Mach line is likely to be negligible due to the smallness of η.

b) Patching Mach Line

The differential equation for the patching Mach line, Equation (2.55), was calculated and is plotted in Figures 3.10 and 3.11. The former shows the relative importance of the various powers of η. It is fortunate that the very lengthy η^3-term appears to be completely negligible.

The patching Mach line itself was determined by means of the series approximation, Equation (2.61). This series becomes

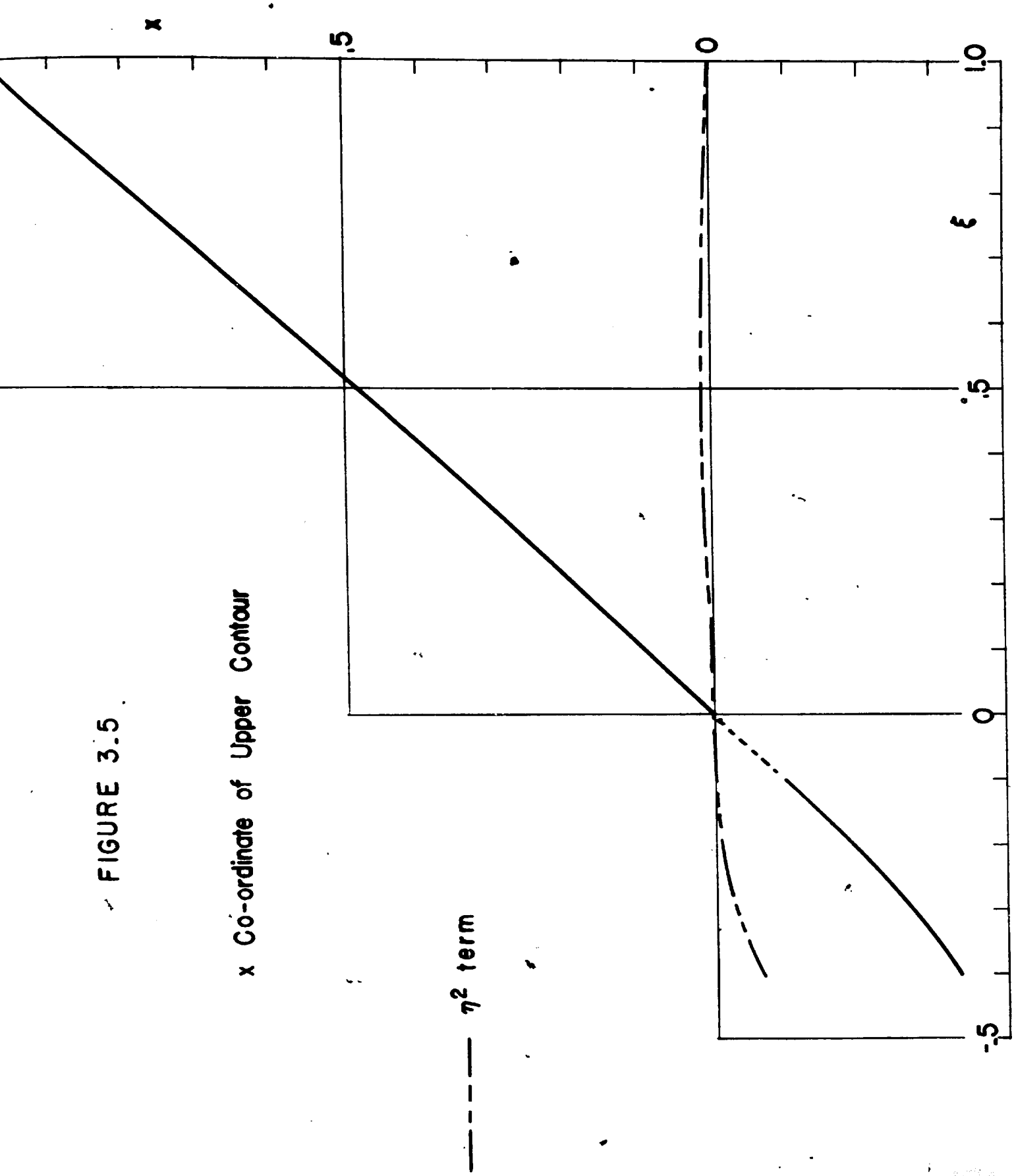


FIGURE 3.5

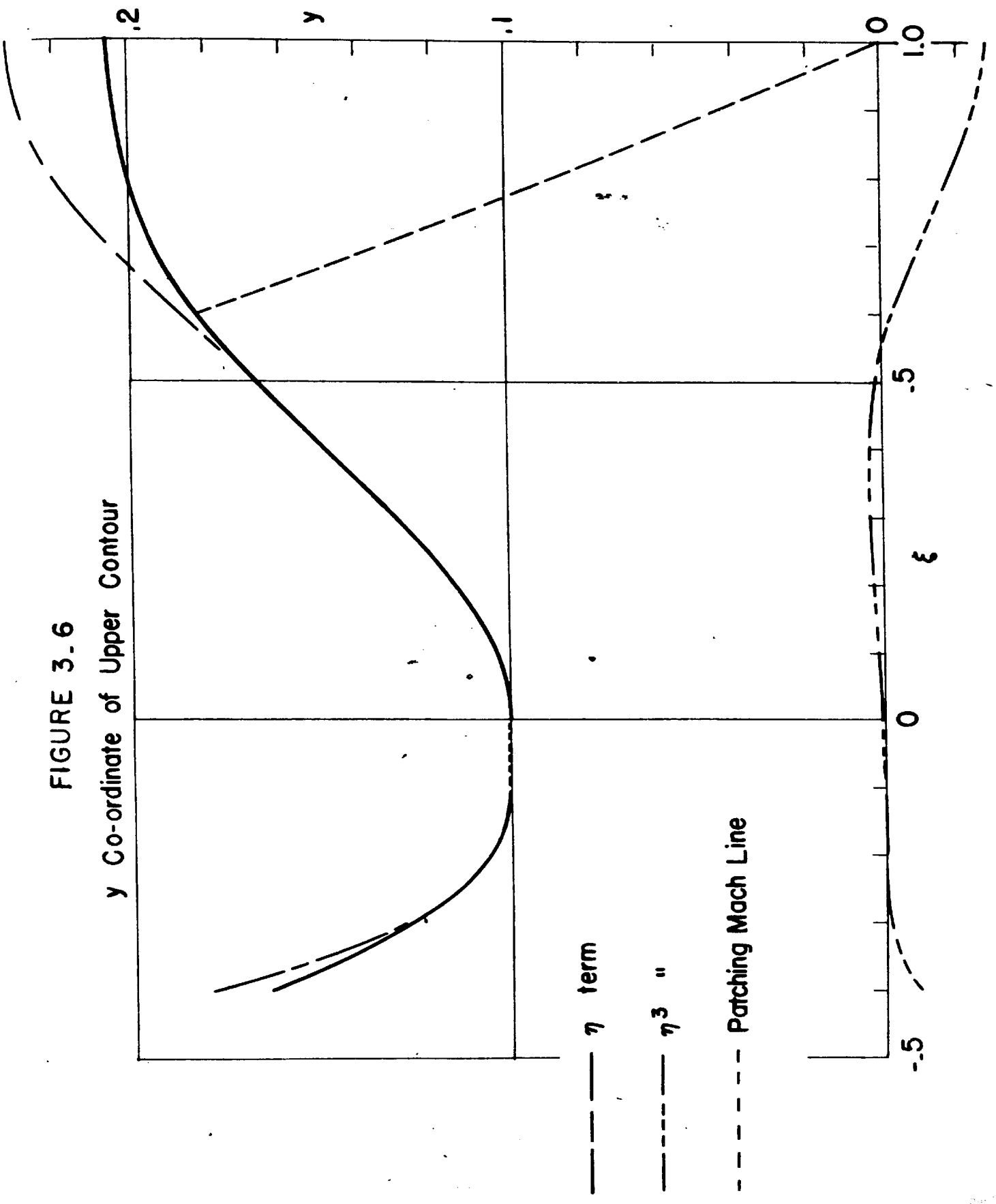


FIGURE 3.6
y Co-ordinate of Upper Contour

FIGURE 3.7

Upper to Lower Wall Pressure Ratio

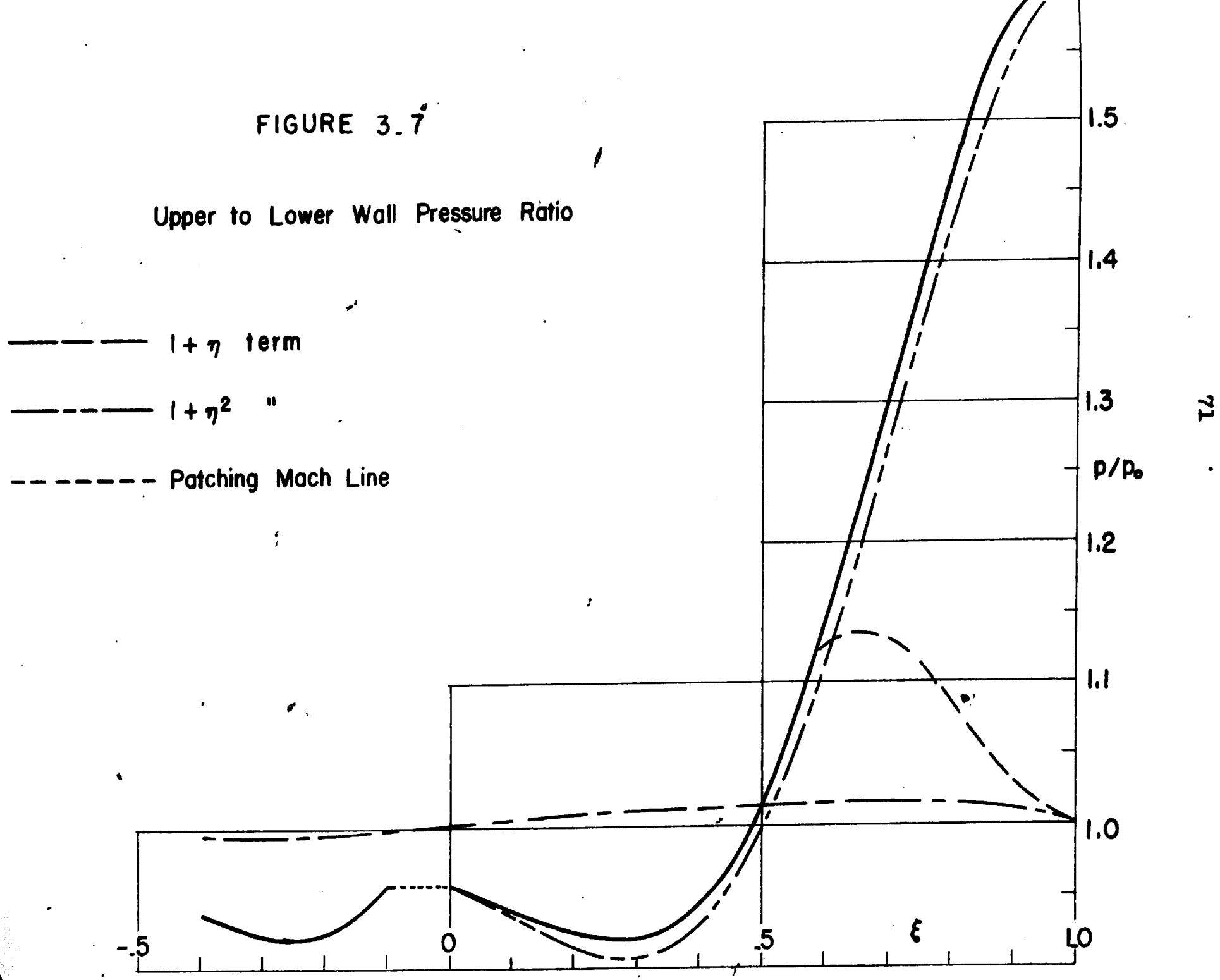


FIGURE 3.8

Speed Ratio Along Upper Contour

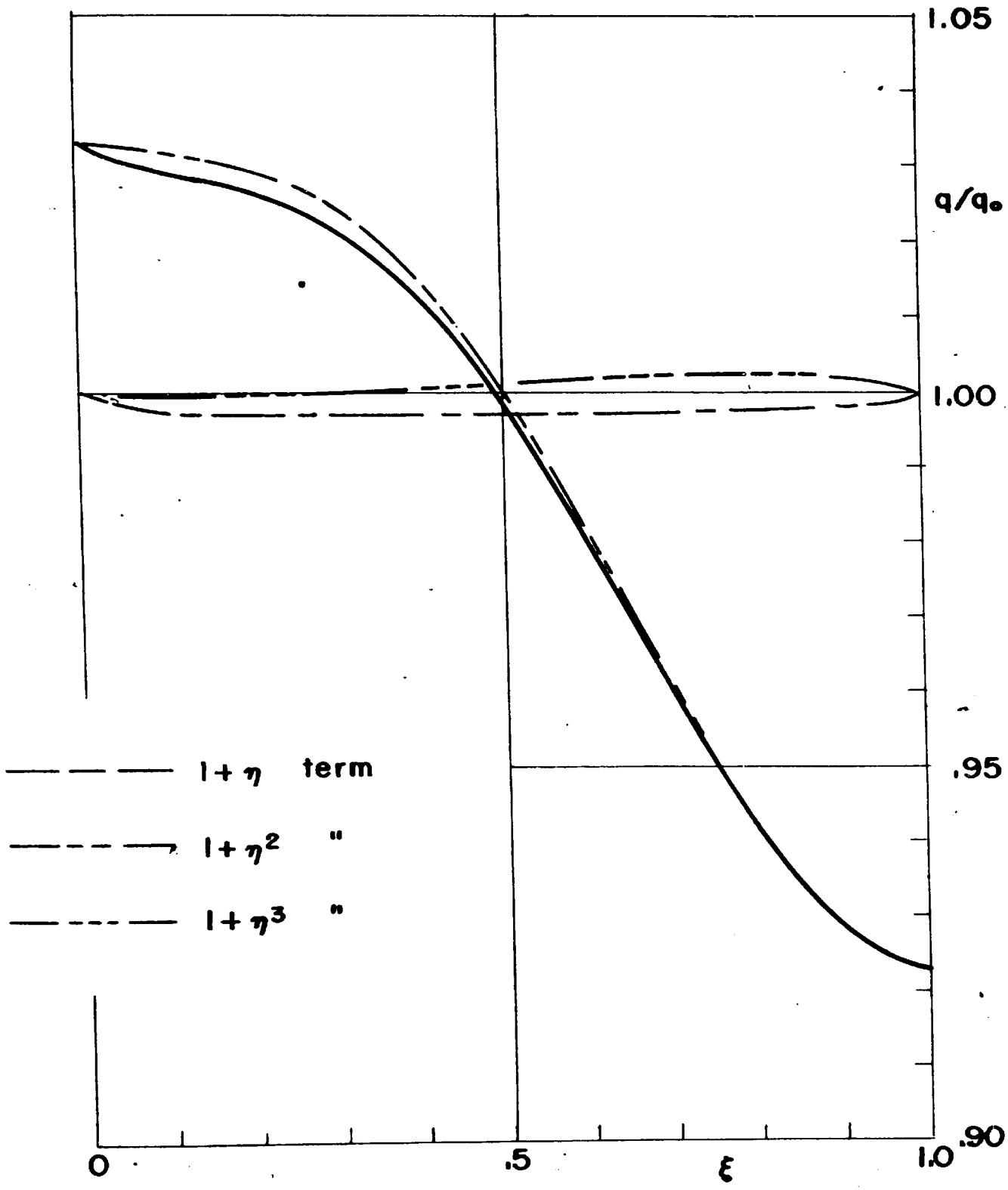


FIGURE 3.9

Flow Direction Along Upper Contour

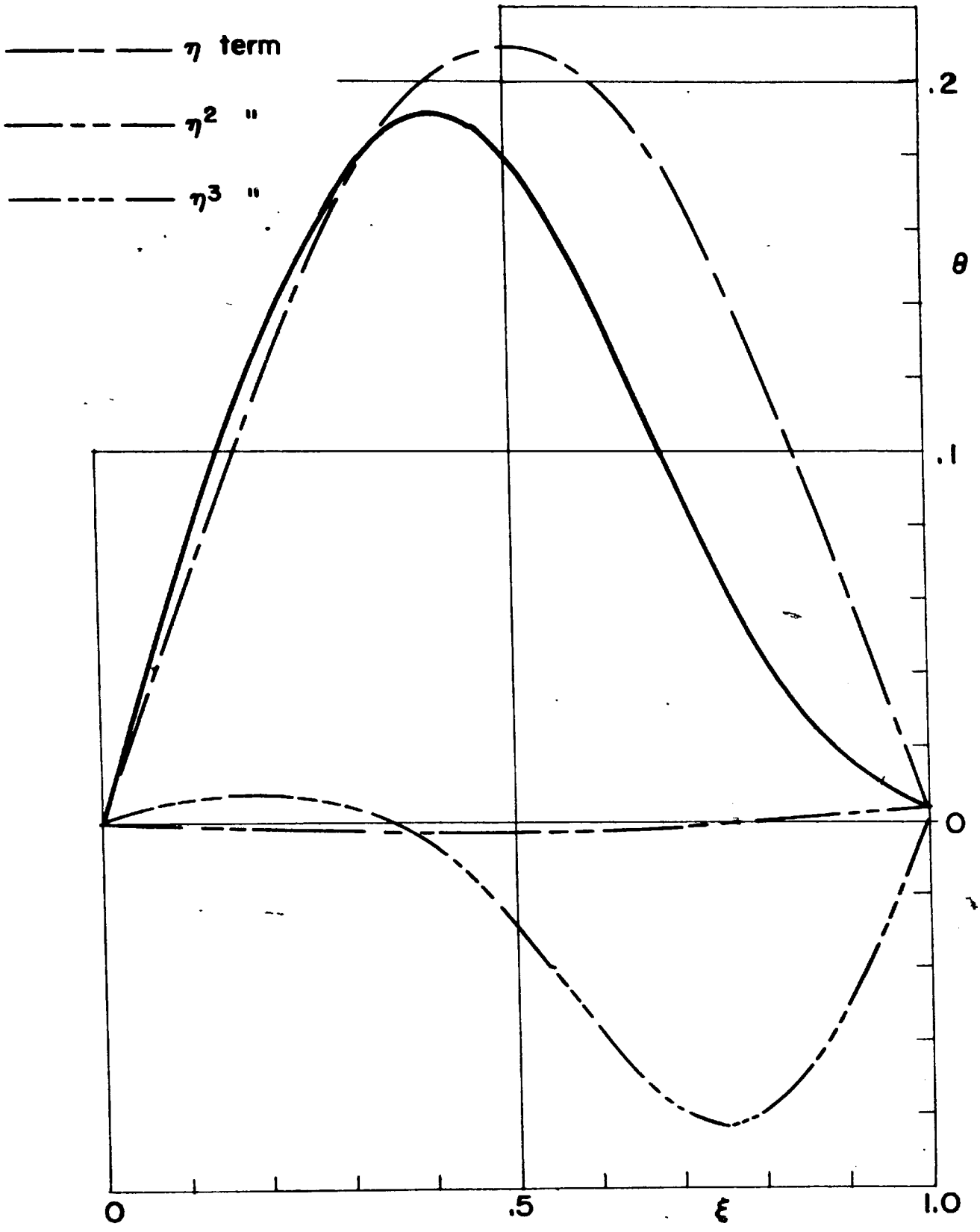


FIGURE 3.10

η – Terms of Patching Mach Line Equation

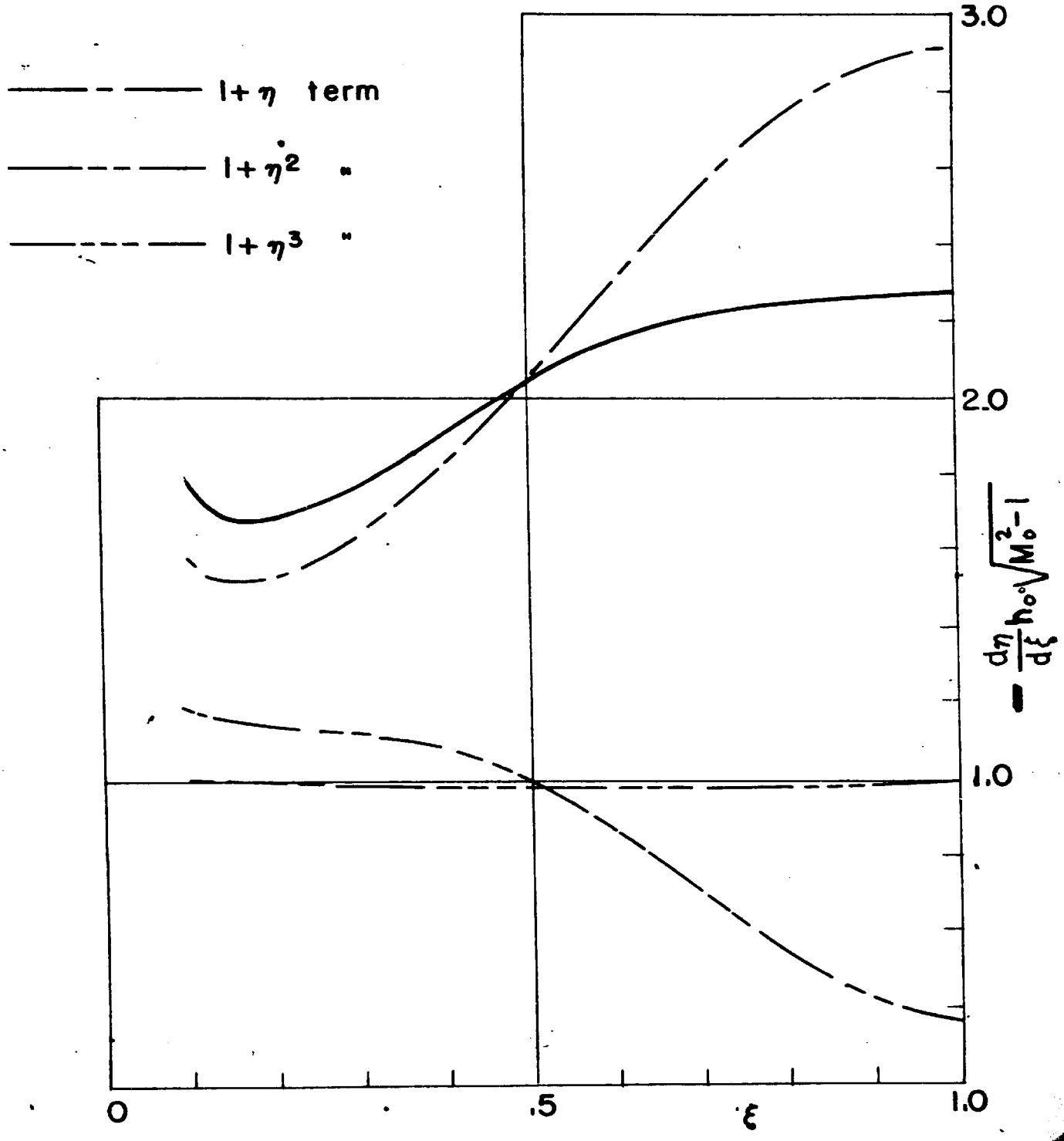
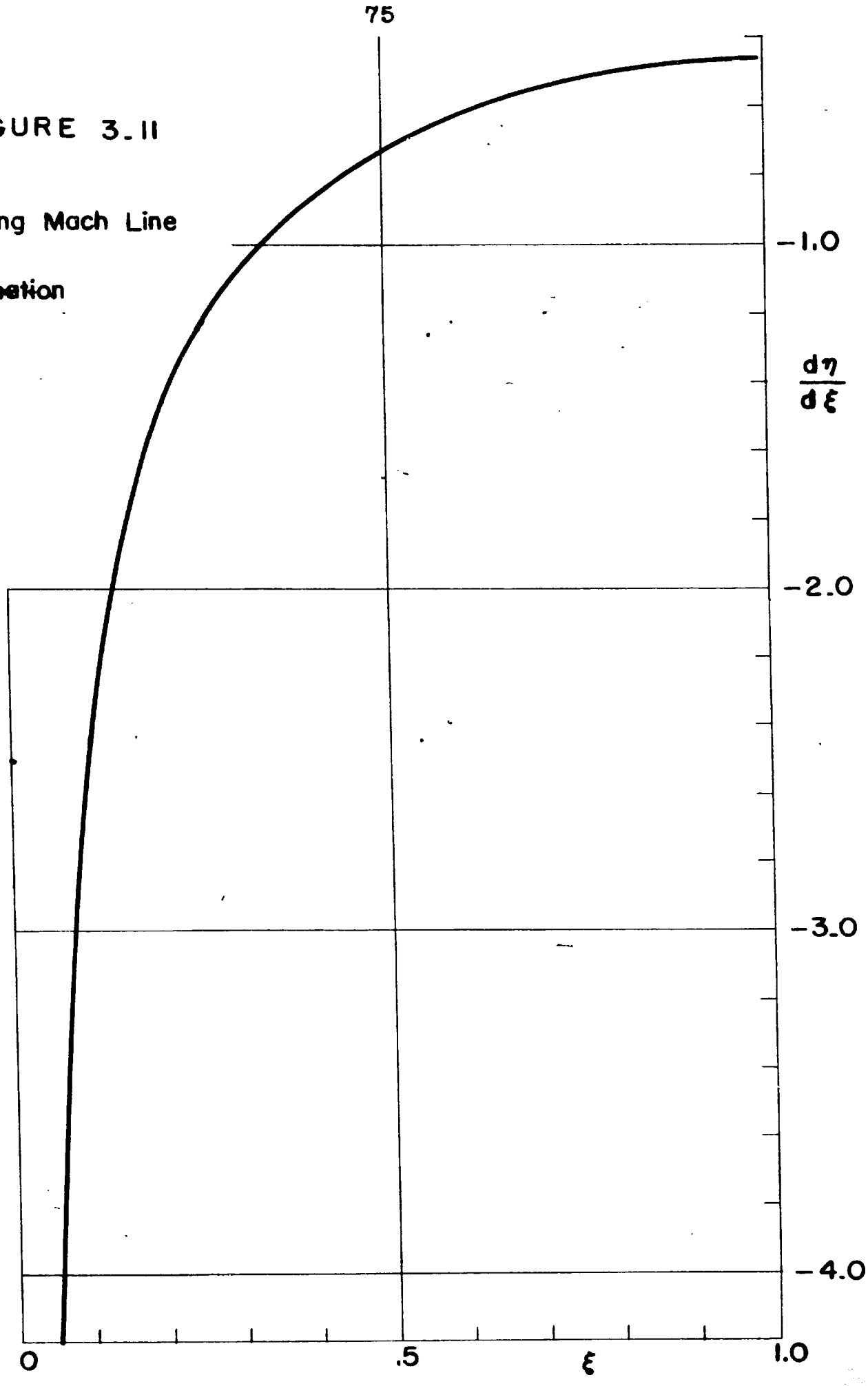


FIGURE 3_11

Patching Mach Line

Equation



$$\xi = 1.0 - 5.024\,\eta + 99.547\,\eta^3 .$$

After suitable values of ξ have been selected between 1.0 and, say, .50, the corresponding η-values are used in equations (2.41), (2.42), (2.46), and (2.44) to calculate x, y, p/p_o and Θ for the patching Mach line. These y and p/p_o values are also shown in Figures 3.6 and 3.7 respectively.

c) Recompression Contour

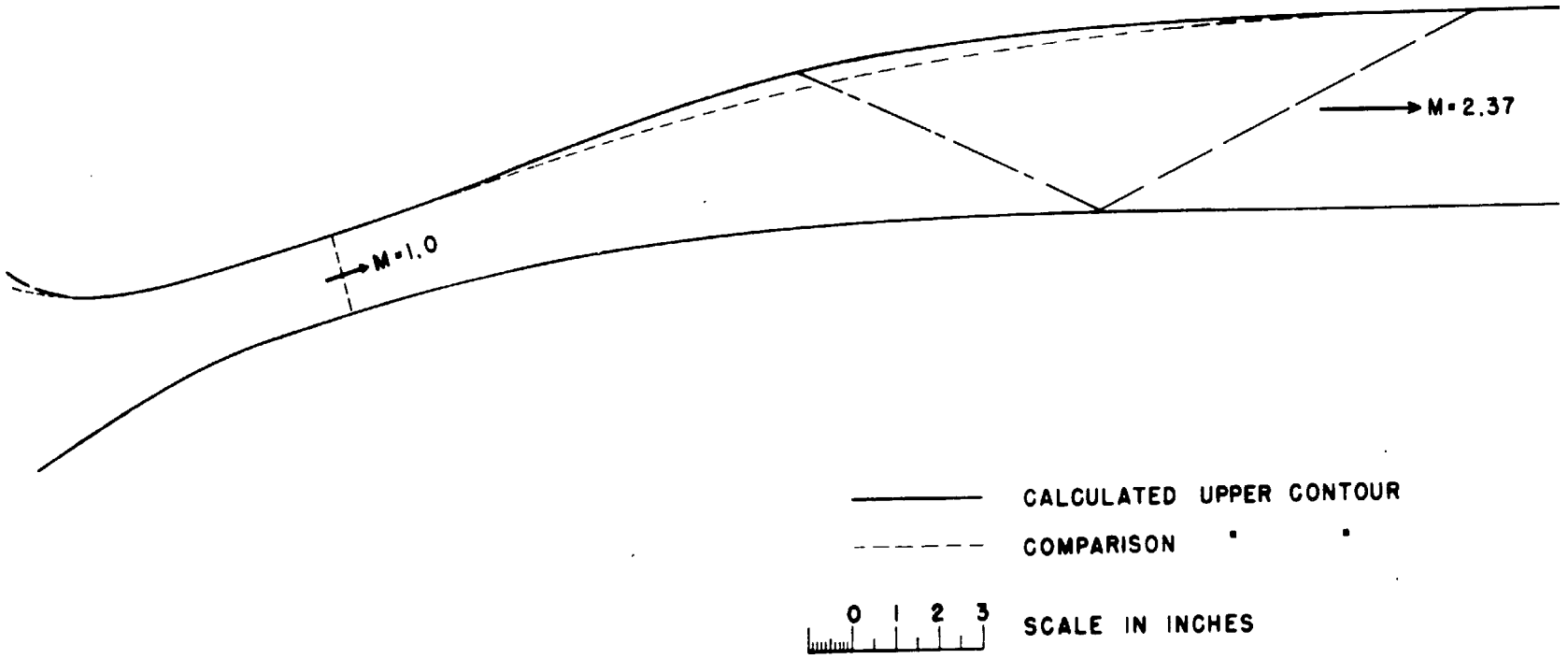
Once x, y, p/p_o and Θ for the patching Mach line have been obtained, the nozzle contour for the simple wave region can be calculated from equation (2.64).

d) Complete Nozzle Contours

The complete nozzle contour can now be drawn and is shown in Figure 3.12 together with the comparison contour.

FIGURE 3.12

CALCULATED AND COMPARISON NOZZLE CONTOURS



CHAPTER IV

DESIGN MACH NUMBER CHANGE THROUGH CONTOUR TRANSLATION

It has been shown experimentally that an asymmetric curved nozzle can be used to vary the design Mach number by a simple translation of one contour with respect to the other. This translation would in general be parallel to the test section axis. Such nozzles have been designed by the method of characteristics and a rather lengthy process of iteration. The question arises: Is it possible to derive relations for the analytic nozzle design method to include the Mach number variation by means of translation, or is an iteration method indicated.

Suppose one has to design a nozzle for a range of design Mach numbers from M_{D_1} to M_{D_2}. The relative translation is found easily from Figure 4.1 and is

$$d = t(\cot\alpha_2 - \cot\alpha_1) = t\left(\sqrt{M_{D_2}^2-1} - \sqrt{M_{D_1}^2-1}\right). \quad (4.1)$$

No difficulty is experienced in determining a nozzle for, say, M_{D_1} after choosing a convenient and continuous h_o-distribution and calculating an upper contour for a constant η_{C_1}. Now consider this η_{C_1} contour translated through a distance d to give, supposedly, a design Mach number M_{D_2}. The η-value of this translated contour is also known since from equations (2.14) and (2.16)

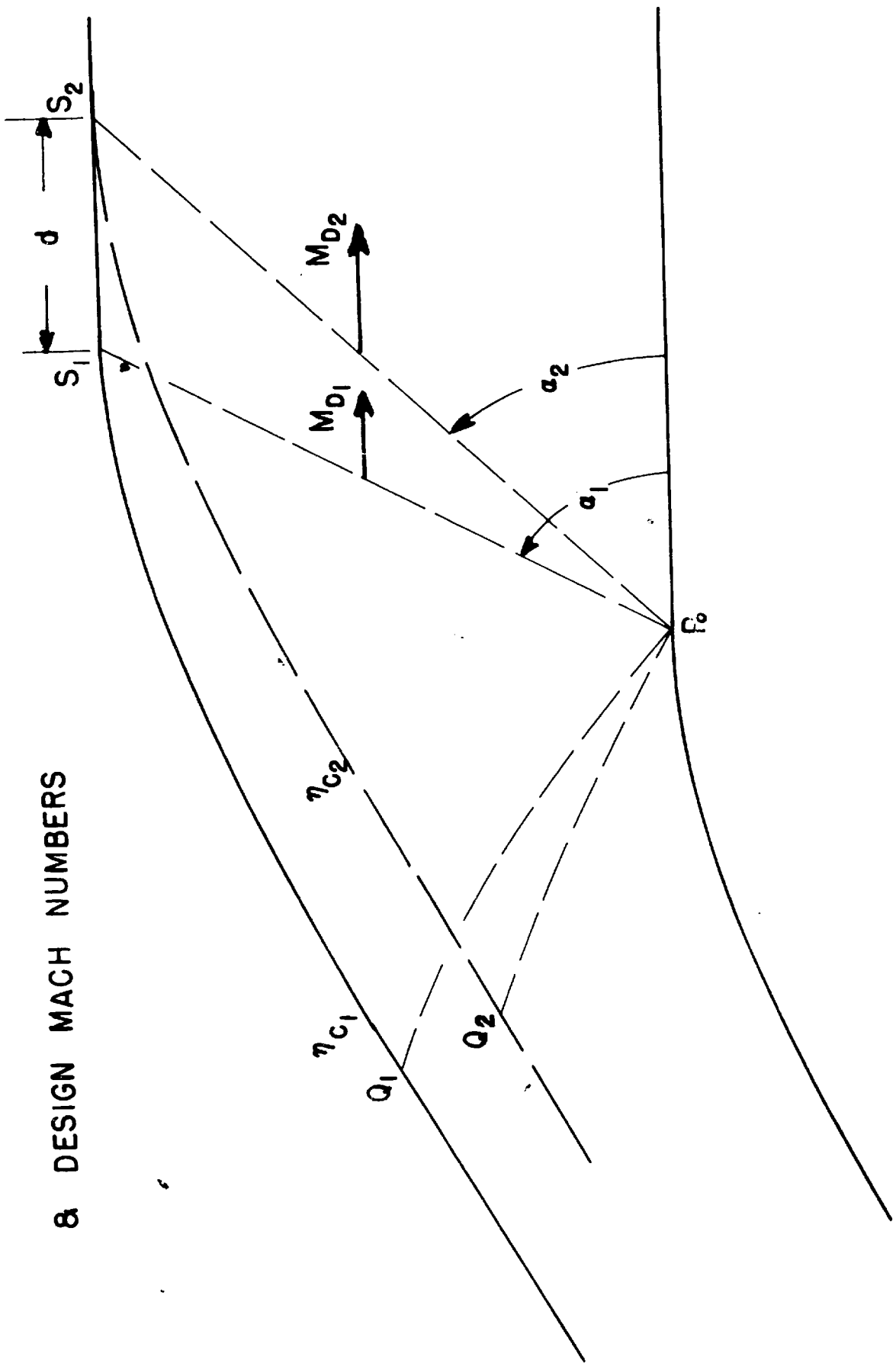


FIGURE 4.1

RELATION BETWEEN NOZZLE TRANSLATION & DESIGN MACH NUMBERS

$$\eta_C = \frac{\psi_D}{\rho^* q^*} = \frac{\rho_D q_D t}{\rho^* q^*} = \frac{t}{h_{o_D}} \quad ;$$

and hence

$$\eta_{C_2} = \frac{t}{h_{o_{D_2}}} \quad . \tag{4.2}$$

This η_{C_2} - streamline contour, obtained by translating the η_{C_1} -contour, is supposed to give a uniform M_{D_2}-flow. In order to verify this, one would have to solve the boundary value problem for equations (2.7) and (2.8) with prescribed streamline η_{C_2} and given stagnation conditions. This is exactly the problem which has not been solved, and for which the method in Chapter II was developed. Thus one is unable to determine the flow field under these conditions directly and a process of iteration is required.

Suppose one starts with an assumed h_{o_2}-distribution of the same form as h_{o_1}, but with a design value of h_{oD_2} corresponding to M_{D_2}. After calculating an upper contour with this h_{o_2} function for an η_{C_2}-value one finds that, in general, this contour will not exactly coincide with the η_{C_1}-contour translated through a distance d. The test section height is of course correct and so is the throat; then, if the two h_o-distributions are continuous and have zero slope at the throat and at the start of the test section, continuity of curvature is also assured at the patching Mach lines and the

test section junctures of these contours which are smooth and continuous throughout. The discrepancies between these contours can not therefore be very large and can be approximated by a perturbation term to the h_{o_2}-distribution.

Assume the h_{o_2}-distribution perturbed by a small term $\delta(\xi)$ which is continuous and has small, continuous derivatives δ', and δ''. Substitute

$$\begin{aligned} h_o &= h_{o_2} + \delta , \\ h_o' &= h_o'_2 + \delta' , \\ h_o'' &= h_o''_2 + \delta'' , \end{aligned}$$

into equations (2.41) through (2.46) and neglect products of δ and its derivatives with η^2, η^3, and κ. It is found that the perturbation terms remain only in the y and Θ equations as follows:

$$\begin{aligned} y &= y(h_{o_2}) + \delta\eta , \\ \Theta &= \Theta(h_{o_2}) + \delta'\eta , \end{aligned} \qquad (4.3)$$

where (h_{o_2}) denotes the value due to the unperturbed h_{o_2}-distribution.

It is therefore possible to determine a perturbation function $\delta(\xi)$ from the geometric discrepancies in y and Θ between the η_{C_2}-contour calculated from an h_{o_2}-function and that of the translated η_{C_1}-contour. A second η_{C_2}-contour can now be calculated from the $(h_{o_2} + \delta)$-distribution and compared to the translated η_{C_1}-contour. This process may be repeated until agreement is satisfactory.

If trigonometric functions such as equation (2.66) are used for h_o, the $\delta(\xi)$ function will conveniently be

trigonometric also. The iteration process outlined above is briefly summarized below and shown in Figure 4.2.

1) Calculate contour 1 from $h_{o_1} = a_1 + b_1 \sin \pi (\xi + C_1)$ and η_{C_1} for M_{D_1}.

2) Calculate contour 2 from $h_{o_2} = a_2 + b_2 \sin \pi (\xi + C_1)$ and η_{C_2} for M_{D_2}.

3) Translate contour 1 in X-direction through distance d into contour 2'.

4) From $\Delta y = \delta \eta_{C_2}$ and $\Delta \Theta = \delta' \eta_{C_2}$ between contours 2 and 2' determine a perturbation of the form $\delta = d \sin \pi (\xi + C)$.

5) Calculate a new contour 3 from $(h_{o_2} + \delta)$ and η_{C_2}.

6) Repeat steps 4) and 5) until contour 2' and contour from last perturbation are within acceptable agreement.

Since Δy and $\Delta \Theta$, and therefore δ, and δ', will be small, this iteration will converge in a few cycles. If the method of characteristics is used in the design of such a variable Mach number nozzle, about 10 or more iterations are required (Reference 2).

It should be noted that the relation between the perturbation δ and the initial contour discrepancies Δy and $\Delta \Theta$ (Equation 4.3) holds only in the nozzle region II (see Figure 1.1), i.e. between the throat and the patching Mach line. The recompression contour (region III) is uniquely determined only by the geometry of the patching Mach line and the flow properties along it, and cannot be related explicitly to the contour of region II. This dilemma is greatly alleviated if the nozzle incorporates continuous wall curvature at points Q and S, (Figure 4.1), i.e. if h_{o_B}' and $h_{o}'_{D} + \delta'$ vanish at point P_o (cf. Chapter II, Section 5). One is then assured of

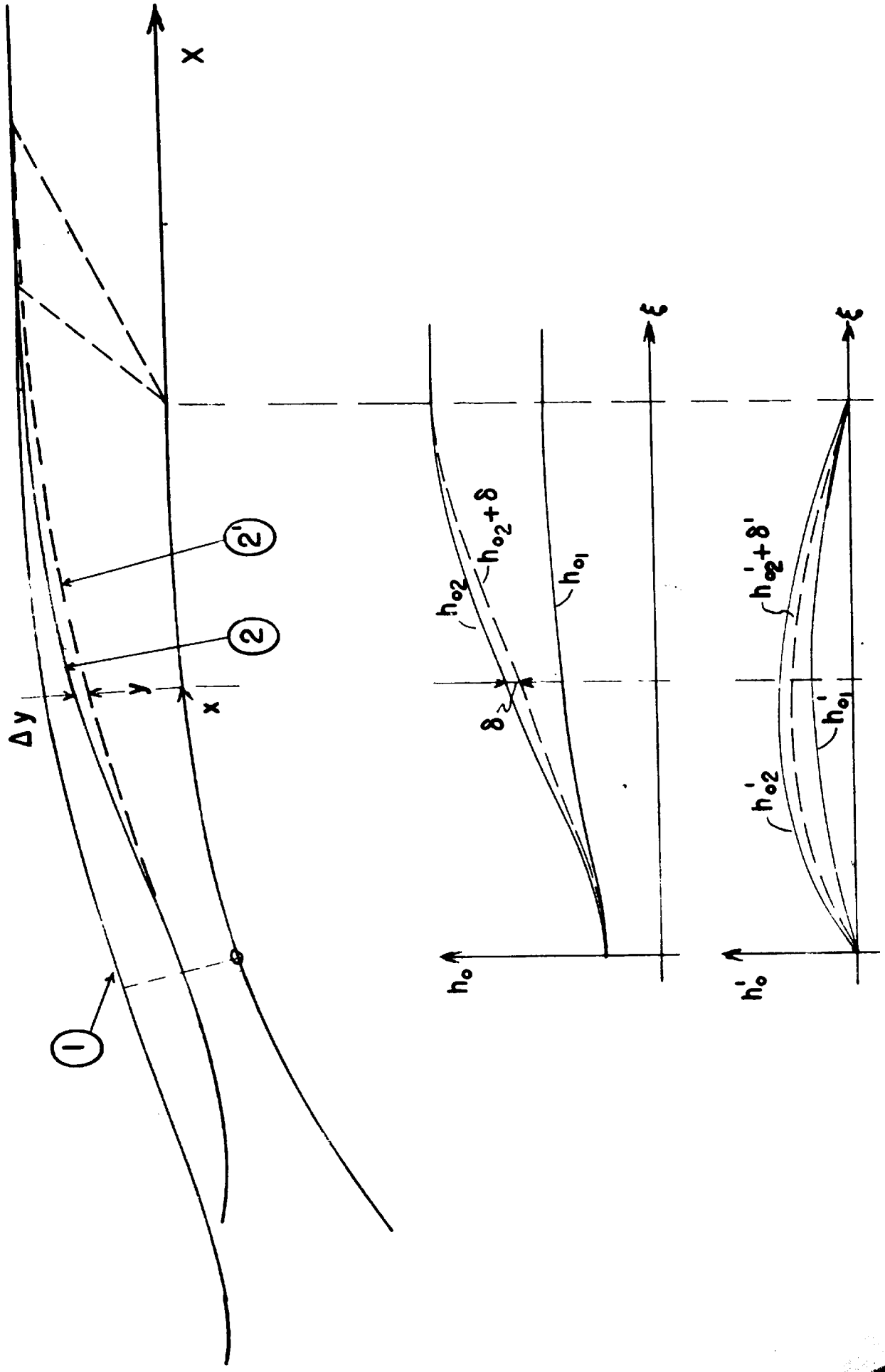


FIGURE 4.2

NOZZLE CONTOURS & h_o- FUNCTIONS FOR ONE ITERATION

having continuous curvature and slopes at the end points Q and S of the recompression region. Furthermore, point S is geometrically fixed by the design Mach wave and the test section height, point Q is approximately located through equation (2.61), and the recompression contour is a smooth curve through these points. Although theoretically an infinite number of recompression contours could exist, the above conditions considerably limit the number of curves suitable for a variable Mach number nozzle and only a few iterations of the type described above will be needed to arrive at the proper contour.

An interesting consequence of this discussion is the following possibility. If the mechanical design of the nozzle permits contour adjustments by means of a flexible plate and jacks, such flexibility is required only in the recompression region corresponding to the highest design Mach number. The remainder of the nozzle can be fabricated from solid blocks and need not be changed regardless of the lower design Mach number. Nevertheless, the considerations of continuous wall curvature and smooth contour should not be violated, otherwise even a flexible recompression contour (which insists on continuous wall curvature) would not be able to cancel exactly all expansion waves and a non-uniform test section flow would result.

CHAPTER V

BOUNDARY LAYER CORRECTION METHODS

1. Introduction

After designing a two-dimensional asymmetric nozzle by the perfect fluid theory of the preceeding chapters, one must decide what do do, if anything, to account for boundary layer growth along the walls of the nozzle. The purpose of such boundary layer corrections is, of course, to assure supersonic flow of the exact design Mach number and of uniform quality, i.e. without gradients or shock- or expansion disturbances caused by viscous effects.

The actual performance of a variety of supersonic nozzles has indicated that it is quite satisfactory to "open up" the contoured nozzle walls by an amount equal to the displacement thickness. There have also been many entirely satisfactory nozzles in the lower Mach number range which have had no viscous corrections at all. Such uncorrected nozzles gave, of course, a Mach number lower than the design value but no detectable disturbances were caused by viscous effects.

This experience has led to a widely accepted design philosophy that nozzles for Mach numbers up to about three need not be corrected for viscous effects, but nozzles for higher Mach numbers should be corrected. There has been no systematic experimental evidence to substantiate this rule and no account is taken of the strong Reynolds number effects of

the stagnation state nor the Mach number gradients along the walls of the nozzle under consideration. An attempt is therefore made in the next section to suggest a more valid criterion for the application or non-application of boundary layer corrections.

It is also known that secondary boundary layer flows exist in two-dimensional supersonic nozzles. At the present time no theoretical guidance nor systematic experimentation is available to predict these effects even for symmetrical nozzles. Nearly all boundary layer corrections are presently based on the concept of satisfying continuity of mass-flow by means of displacement thickness corrections. It is implied thereby that the outer edge of the displacement thickness is the effective contour instead of the perfect fluid contour determined from non-viscous theories. References 18 and 19 present the most useful material on this matter including tabulated functions which greatly facilitate boundary layer calculations. The viscous corrections for asymmetric curved nozzles will be based upon this concept and the use of these references.

2. A Criterion For the Application of Boundary Layer Corrections

Boundary layer displacement thicknesses have been given in Reference 2 for both contours of a variable Mach number asymmetric nozzle operating from atmospheric stagnation conditions. This nozzle was designed by the method of characteristics which was iterated to cover the Mach number range

from 1.4 to 4.0. The Mach number gradients along the walls of this nozzle were smooth, as can be seen in Figure 3.3 for Mach 2.37, and are believed similar to those obtainable by the analytic nozzle design method of Chapter II.

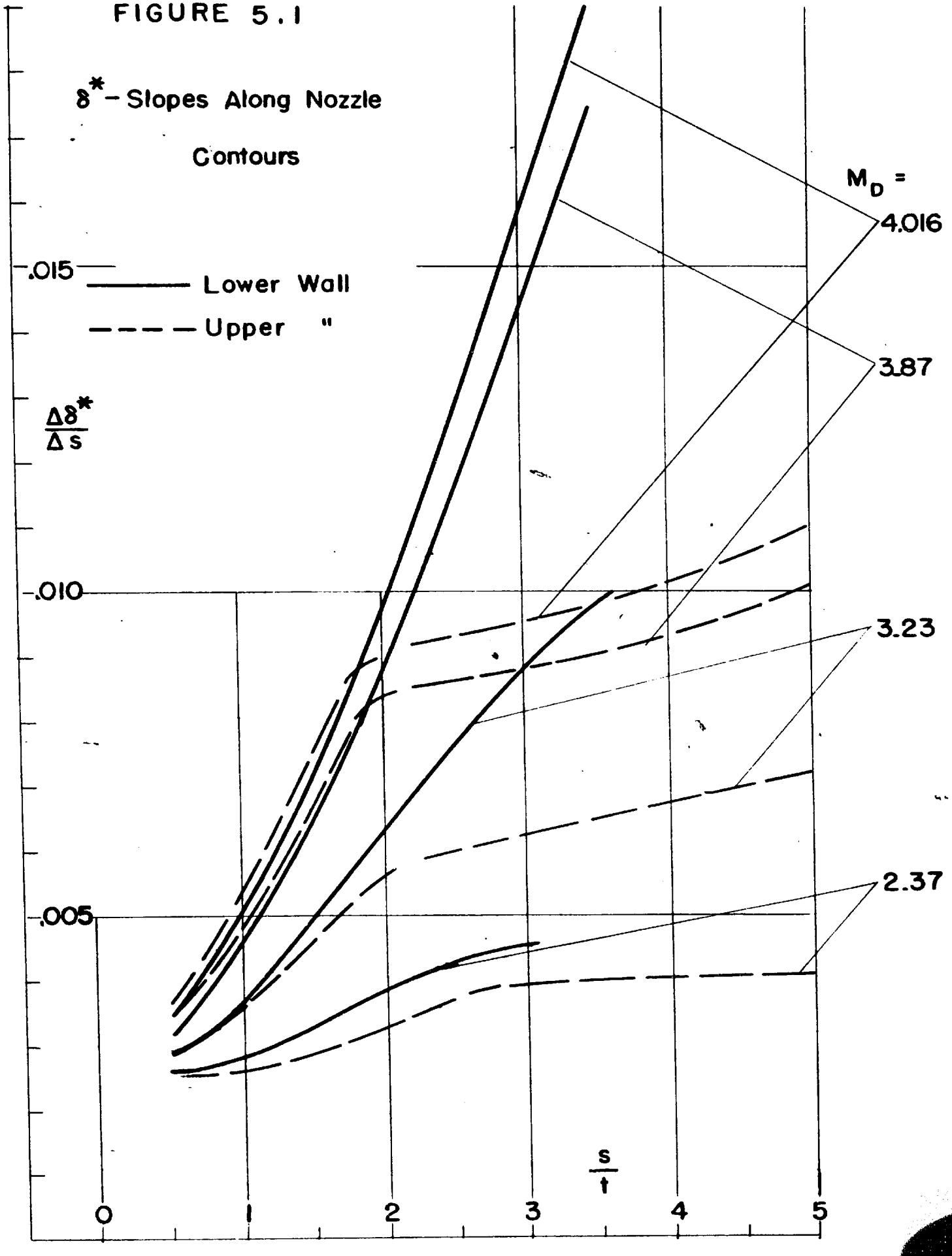
The boundary layer data of Reference 2 has been used to calculate the slope $\Delta \delta^*/\Delta s$ of the displacement thickness for Mach numbers 2.37, 3.23, 3.87, and 4.016. These displacement thickness slopes are plotted in Figure 5.1 against the ratio of contour arc length to test section height. The δ^*-slope is of course taken with respect to the tangent to the perfect fluid contour $Y = F(X)$.

It is clear from this figure that the δ^*-slopes of both walls are smooth and of the same order of magnitude for design Mach numbers up to about three. Above Mach three the slopes on upper and lower walls begin to differ by an amount which increases with increasing Mach number. Furthermore, the upper contour slope tends towards a sudden change near the point of the patching Mach line, although the Mach number distributions along this wall are rather smooth and continuous.

If one considers the boundary of the displacement thickness as the effective contour of the nozzle, the above high Mach number phenomena have considerable meaning.

First, the abrupt change in the δ^*-slope at the upper patching Mach line is essentially a discontinuity in the δ^*-curvature at that point. Since δ^* is considered the effective wall, there exists then a discontinuity in the wall curvature. It was shown in References 14 and 15 that continuous wall

FIGURE 5.1


δ* – Slopes Along Nozzle Contours
Lower Wall
Upper "
$\frac{\Delta\delta^*}{\Delta s}$
.015
.010
.005
M_D =
4.016
3.87
3.23
2.37
0
1
2
3
4
5
$\frac{s}{t}$

curvatures can be incorporated in a nozzle design and are to be favored. Since such considerations of curvature should, of course, apply to the effective contour, it is concluded that some boundary layer correction should be made whenever a strong change in $\Delta \delta^*/\Delta s$ occurs as, for instance, at the two highest Mach numbers of Figure 5.1.

Second, the differences in δ^*-slopes, between upper and lower contours, above Mach three are of sufficient magnitude to suspect noticeable effects on static pressure and Mach number values in the test section. The effect of local slope changes of a perfect fluid contour was shown in Figure 1.3. According to this Figure a slope change of .002 corresponds to a local change in pressure and force coefficient of about 1%. The changes in effective slope due to δ^* are considerably greater than .002, as can be seen from Figure 5.1, and a correspondingly larger effect on the flow properties must be suspected.

On the basis of this discussion it is suggested that the occurrence of strong changes in δ^*-slopes and the magnitude of the related difference in δ^*-slope on opposite contours be used as a criterion to decide if boundary layer corrections are to be applied or not.

With the tables of Reference 19, the calculation of δ^* and $\Delta \delta^*/\Delta s$ is no longer a time-consuming chore. The resulting curves of the displacement thickness slopes along each contour will show at once if boundary layer corrections are needed. Since the procedure includes considerations of

stagnation state and Mach number gradients, it is believed to be more realistic than the crude philosophy mentioned before, of "no corrections" below Mach three.

3. Boundary Layer Corrections For Asymmetric Curved Nozzles

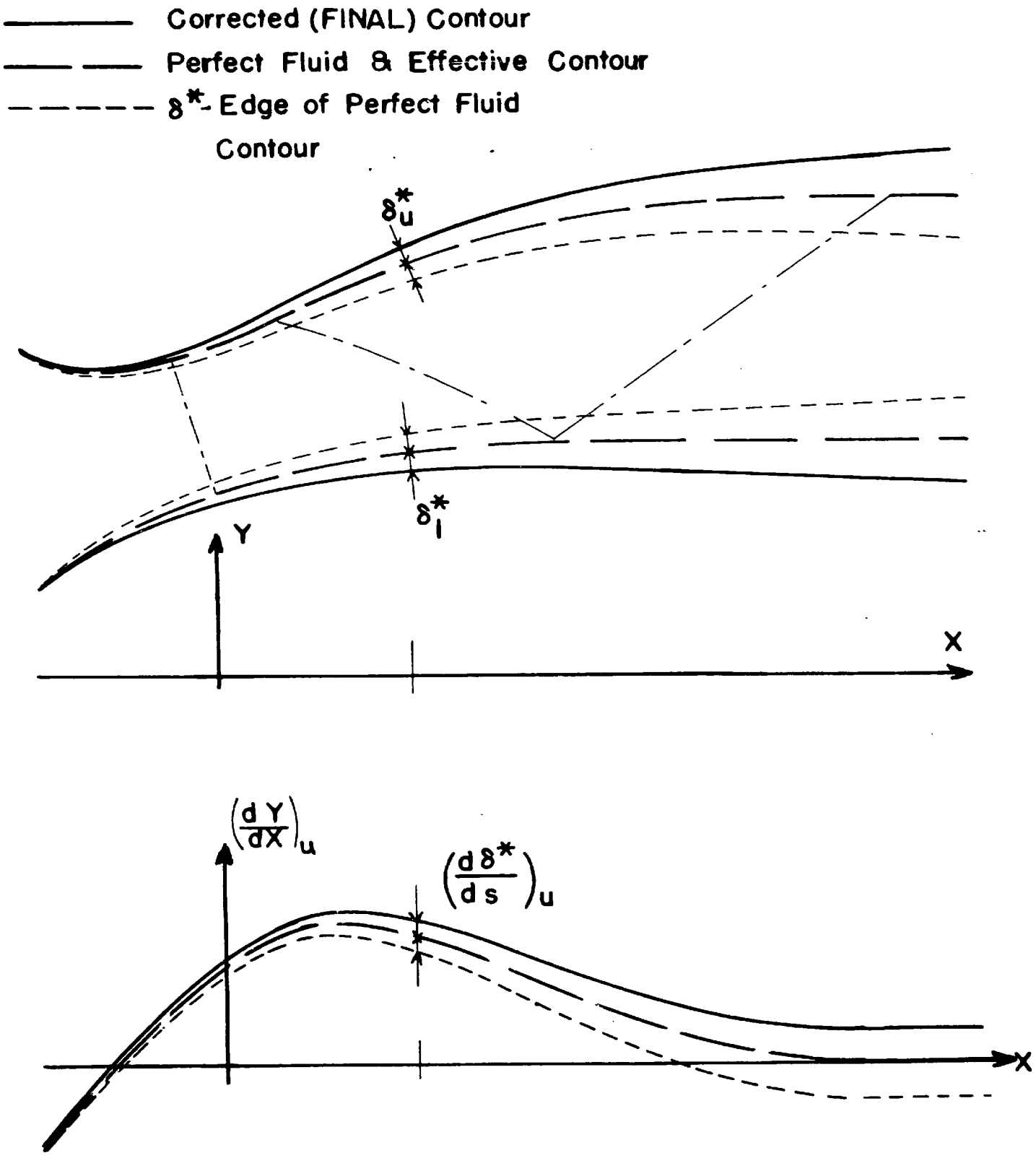
Actual boundary layer corrections can be applied quickly once their need has been determined on the basis of the above criterion. No additional δ^*-calculations are needed since all necessary data was calculated from Reference 19 in the application of the criterion.

It was mentioned in the introduction to this chapter that the generally accepted correction procedure consists of increasing the perfect fluid contours by the δ^*-values at each station. It follows from the discussion of the criterion that the slope of the corrected contour should differ from that of the perfect fluid contour by $\Delta\delta^*/\Delta s$. Consideration of the δ^*-slopes can be a powerful checking procedure or it may be considered a second correction step. In this manner the continuity of mass flow is assured through the corrections to the perfect fluid contour ordinates y, i.e. the actual exit Mach number will be equal to the design Mach number. The additional slope correction, suggested above, will assure the desired angular relation between expansion waves and the effective wall. This is consistent with the concept that the outer edge of the displacement thickness acts as the effective nozzle contour. It is also consistent with the strong effect of contour slope deviations upon the test section flow which was discussed in Chapter I, section 3-a.

The complete boundary layer corrections to an asymmetric curved nozzle are shown schematically in Figure 5.2. The δ^* corrections are most conveniently calculated for each curvilinear abscissa x and can then be applied to the perfect fluid contours as follows: Along the lower contour δ^*_l is equal to the curvilinear corrected contour ordinate (negative) since y is zero. Along the upper contour, $(\delta^*)_u \cos\Theta$ is added to the perfect fluid ordinate y. The corrected Cartesian co-ordinates X_c and Y_c are obtained by adding $\delta^*_l \sin[\omega - (\Delta\delta^*/\Delta s)_l]$ and $-\delta^*_l \cos[\omega - (\Delta\delta^*/\Delta s)_l]$, respectively, to the uncorrected lower contour co-ordinates X and Y. For the upper contour one adds $\delta^*_u \sin[\omega+\Theta+(\Delta\delta^*/\Delta s)_u]$ and $\delta^*_u \cos[\omega + \Theta + (\Delta\delta^*/\Delta s)_u]$, respectively, to its perfect fluid Cartesian co-ordinates.

If such a corrected nozzle is to be designed for an existing test channel with fixed height t, one must estimate the displacement thickness on the upper and lower wall in the center of the test section. This is not too difficult since the arc lengths of the contours are fairly well known. The initial perfect fluid nozzle contours can then be calculated from an h_o-distribution based on the design Mach number and a fictitious test section height $t_o = t - (\delta^*_u + \delta^*_l)$.

FIGURE 5.2



Boundary Layer Corrections

APPENDIX A

TWO-DIMENSIONAL EQUATION OF CONTINUITY AND CONDITION OF IRROTATIONALITY IN CURVILINEAR CO-ORDINATES

1. Continuity Equation

The equation of continuity

$$\operatorname{div}(\rho\vec{q}) = 0 \qquad \text{(A-1)}$$

can be derived for two-dimensional fields in the manner given by Kuethe and Schetzer, Reference 16.

Since

$$\operatorname{div}(\rho\vec{q}) = \lim_{\Delta S \to 0} \frac{\text{Excess Mass Flux}}{\Delta S}, \qquad \text{(A-2)}$$

it is only necessary to write down the net mass flux passing through the sides of an elementary area ΔS expressed in curvilinear co-ordinates, see Figure A-1, and to take the limit as ΔS vanishes.

The excess in x-direction is

$$\left[\rho u + \frac{\partial(\rho u)}{\partial x} dx\right] dy - \rho u dy = \frac{\partial(\rho w)}{\partial x} dx dy, \qquad \text{(A-3)}$$

and in y-direction

$$\left[\rho v + \frac{\partial(\rho v)}{\partial y} dy\right]\left[1+\kappa(y+dy)\right]dx - \rho v(1+\kappa y)dx$$

$$= \rho v \kappa \, dx dy + \frac{\partial(\rho v)}{\partial y}\left[1+\kappa(y+dy)\right]dx dy \, .$$

Therefore

$$\lim_{\substack{dx\to 0 \\ dy\to 0}} \frac{\text{Excess}}{(1+\kappa y)dx dy} = \frac{1}{1+\kappa y}\left[\rho v \kappa + \frac{\partial(\rho v)}{\partial y}(1+\kappa y) + \frac{\partial(\rho u)}{\partial x}\right]$$

$$= \frac{1}{1+\kappa y}\left[\frac{\partial(\rho u)}{\partial x} + \frac{\partial}{\partial y}\left\{(1+\kappa y)(\rho v)\right\}\right].$$

Hence, equation (A-1) becomes

$$\frac{\partial(\rho u)}{\partial x} + \frac{\partial}{\partial y}\left[(1+\kappa y)(\rho v)\right] = 0 \, . \qquad \text{(A-4)}$$

This equation agrees with that given by Goldstein, Reference 10, page 101, for $\alpha = x$, $\beta = y$, $\gamma = 0$, $h_1 = 1 + \kappa y$, $h_2 = 1$.

2. Irrotationality Condition

Irrotational flow requires

$$\text{curl } \vec{q} = 0 \, . \qquad \text{(A-5)}$$

For calculating purposes one can express the curl of the velocity as

$$\text{curl } \vec{q} = \lim_{\Delta S \to 0} \frac{\oint \vec{q} \cdot d\vec{s}}{\Delta S} \quad . \tag{A-6}$$

From Figure A-2 it follows that

$$\oint \vec{q} \cdot d\vec{s} = u(1+\kappa y)dx + (v + \frac{\partial v}{\partial x}dx)dy - v\,dy$$

$$-\left[u + \frac{\partial u}{\partial y}dy\right]\left[1+\kappa(y+dy)\right]dx \;,$$

and

$$\lim_{\substack{dx\to 0 \\ dy\to 0}} \frac{\oint \vec{q} \cdot d\vec{s}}{(1+\kappa y)dx\,dy} = \frac{1}{1+\kappa y}\left[\frac{\partial v}{\partial x} - \kappa u - \frac{\partial u}{\partial y}(1+\kappa y)\right] ;$$

hence

$$\frac{\partial v}{\partial x} - \frac{\partial}{\partial y}\left[(1+\kappa y)u\right] = 0 \quad . \tag{A-7}$$

FIGURE A.1

Mass Flux Through Incremental Area

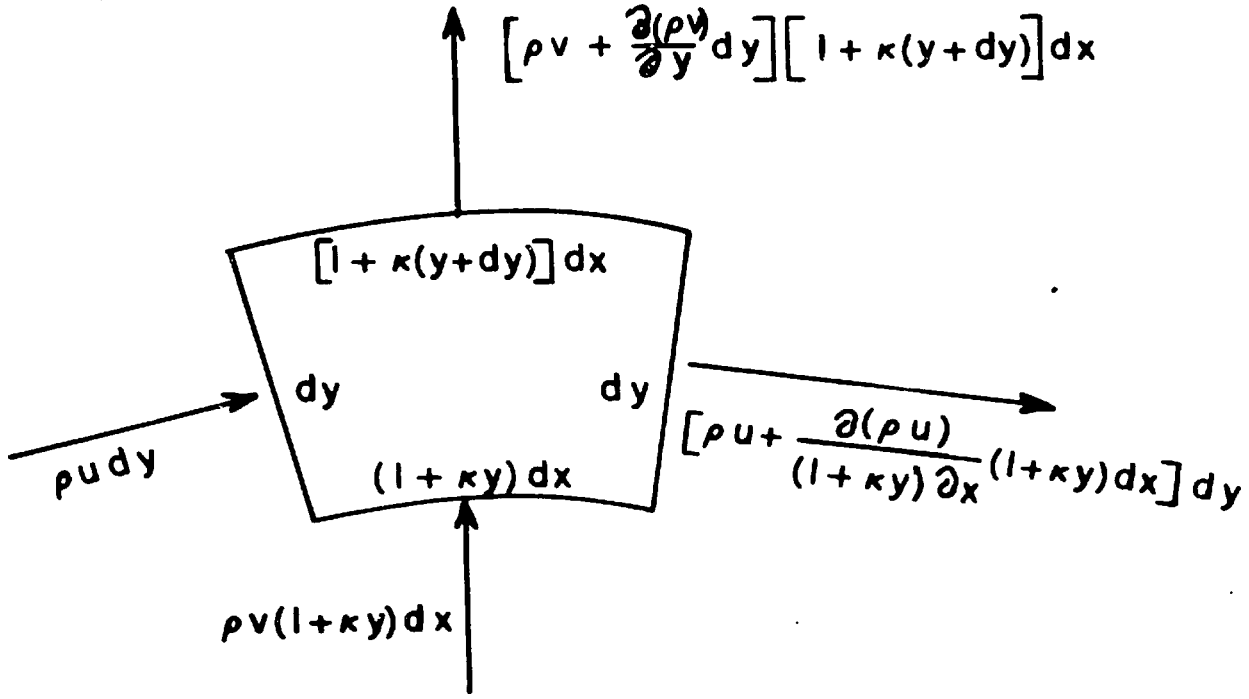
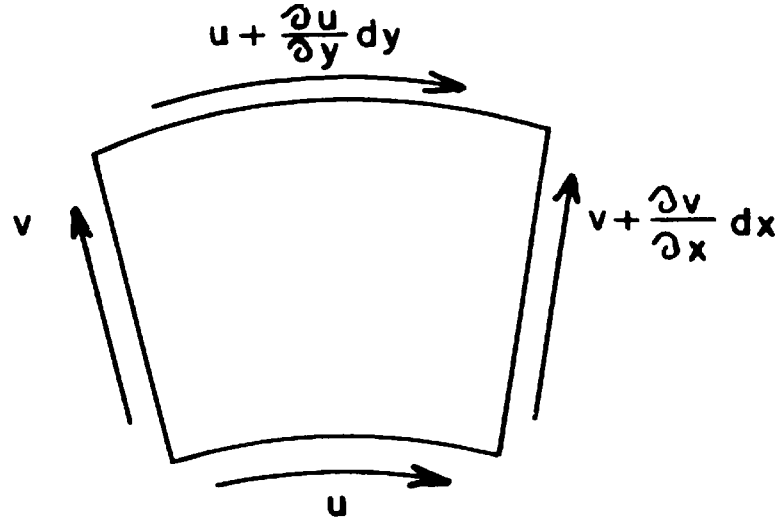


FIGURE A.2

Velocity Components Along Incremental Area



APPENDIX B

CALCULATION OF COEFFICIENTS OF η-SERIES

The set of partial differential equations (2.18), (2.20), (2.23), and (2.24) are assumed to have solutions of the form (2.37) to (2.40). In the subsequent calculations the series will be terminated at the η^3-term, and κ^2-terms will be neglected. Since the equations contain both q and h, their functional relation, equation (2.31), must also be given in series form. This is done first by substituting equation (2.39) into (2.31) term by term and using the binomial theorem.

$$\left(\frac{q}{q_0}\right)^{-1} = 1 - q_1\eta - q_2\eta^2 + (2q_1q_2 - q_3)\eta^3, \quad \text{(B-1)}$$

and

$$\left[\frac{(\gamma+1) - (\gamma-1)\left(\frac{q_0}{q^*}\right)^2\left(\frac{q}{q_0}\right)^2}{(\gamma+1) - (\gamma-1)\left(\frac{q_0}{q^*}\right)^2}\right]^{\frac{-1}{\gamma-1}}$$

$$= \left[\frac{(\gamma+1) - (\gamma-1)\left(\frac{q_0}{q^*}\right)^2\left\{1 + 2q_1\eta + 2q_2\eta^2 + 2(q_1q_2+q_3)\eta^3\right\}}{(\gamma+1) - (\gamma-1)\left(\frac{q_0}{q^*}\right)^2}\right]^{\frac{-1}{\gamma-1}},$$

where q_1^2 - terms have been dropped, since subsequent results give $q_1 = K$ so that q_1^2 is negligible as is K^2. The right hand side can be written as

$$\left[1 - \frac{(\gamma-1)\left(\frac{q_0}{a^*}\right)^2}{(\gamma+1)-(\gamma-1)\left(\frac{q_0}{a^*}\right)^2}\left\{2q_1\eta + 2q_2\eta^2 + 2(q_1q_2+q_3)\eta^3\right\}\right]^{\frac{-1}{\gamma-1}},$$

or, with equation (2.32),

$$\left[1 - \frac{(\gamma-1)M_0^2}{2}\left\{2q_1\eta + 2q_2\eta^2 + 2(q_1q_2+q_3)\eta^3\right\}\right]^{\frac{-1}{\gamma-1}}.$$

This can be expanded into

$$1 + q_1M_0^2\eta + q_2M_0^2\eta^2 + \left\{(q_1q_2+q_3)M_0^2 + \gamma q_1q_2M_0^4\right\}\eta^3. \quad \text{(B-2)}$$

Hence, multiplication of (B-1) and (B-2) gives

$$\frac{h}{h_0} = 1 + q_1(M_0^2-1)\eta + q_2(M_0^2-1)\eta^2 + \left\{q_1q_2(\gamma M_0^4 - M_0^2 + 2) + q_3(M_0^2-1)\right\}\eta^3. \quad \text{(B-3)}$$

Now all terms in the differential equation can be expanded and collected in like powers of η. This process leads to the following set of equations:

From equation (2.18)

η^0-term : $x_1 = 0$.

η -term : $2x_2 = -h_0\Theta_1$.

η^2-term: $3x_3 = -h_0[\Theta_2 - Ky_1\Theta_1 + (M_0^2-1)q_1\Theta_1]$.

η^3-term: $4x_4 = -h_0[\Theta_3 - \frac{\Theta_1^3}{6} - Ky_1\Theta_2 + \Theta_2 q_1(M_0^2-1) + q_2\Theta_1(M_0^2-1)]$.

From equation (2.20)

η^0-term: $y_1 = h_0$.

η-term: $2y_2 = h_0(M_0^2-1)q_1$.

η^2-term: $3y_3 = h_0(M_0^2-1)q_1 - h_0\frac{\Theta_1^2}{2}$.

η^3-term: $4y_4 = h_0[(6M_0^4 - M_0^2+2)q_1q_2 + (M_0^2-1)q_3 - \Theta_1\Theta_2 - (M_0^2-1)\frac{q_1\Theta_1^2}{2}]$.

From equation (2.23)

η^0-term: $q_1 = -Ky_1$.

η -term: $-2q_2 - 2Ky_2 + Kq_1y_1 = -h_0\Theta_1'$.

η^2-term: $-3q_3 + 6q_1q_2 + Kq_2y_1 + K\Theta_1^2y_1 - 3Ky_3$

$= -h_0[\Theta_2' - \Theta_1(Ky_1)' + \Theta_1'(M_0^2-1)q_1]$.

From equation (2.24)

η^0-term: $\Theta_1 = h_0'$.

η-term: $2\Theta_2 + \kappa y_1 \theta_1 - q_1 \theta_1 = (M_0^2-1) q_1 h_0' + 2 h_0 M_0 M_0' q_1 + (M_0^2-1) h_0 q_1'$.

η^2-term: $3\Theta_3 + \kappa \Theta_2 y_1 - 2 q_1 \theta_2 - q_2 \theta_1 = (M_0^2-1) q_2 h_0' + 2 h_0 q_2 M_0 M_0' + h_0 (M_0^2-1) q_2'$.

In these and subsequent equations the term $M_0 M_0'$ is needed. This can be obtained by differentiating equation (2.33) with respect to ξ, i.e.

$$h_0' = \frac{2 h_0 M_0 M_0' (M_0^2-1)}{M_0^2 \{2 + (\gamma-1) M_0^2\}} , \qquad \text{(B-4)}$$

which gives

$$M_0 M_0' = \frac{h_0' M_0^2 \{2 + (\gamma-1) M_0^2\}}{2 h_0 (M_0^2-1)} . \qquad \text{(B-5)}$$

Solving the above 14 equations simultaneously for the unknown q_i, Θ_i, x_j, y_j (where i = 1, 2, 3; j = 1, 2, 3, 4) leads to the results given below for the coefficients of the desired η-series. It should be noted that equations (2.17) and (2.19) serve as checks for these coefficients.

$$q_1 = -\kappa h_o \quad ,$$

$$q_2 = \frac{h_o h_o''}{2} \quad ,$$

$$q_3 = -\frac{\kappa h_o h_o'^2}{6(M_o^2-1)^3}\left[\gamma(\gamma+1)M_o^8 - (2\gamma^2-1)M_o^6 - 3\gamma M_o^4 - 3M_o^2 + 1\right]$$

$$- \frac{\kappa h_o^2 h_o''}{6(M_o^2-1)}\left[(\gamma+4)M_o^4 - M_o^2 - 2\right]$$

$$- \frac{\kappa' h_o^2 h_o'}{3(M_o^2-1)}(\gamma+1)M_o^4$$

$$- \frac{\kappa'' h_o^3 (M_o^2-1)}{6} \quad . \qquad \text{(B-6)}$$

$$\theta_1 = h_o' \quad ,$$

$$\theta_2 = -\frac{\kappa h_o h_o'}{2(M_o^2-1)}(\gamma+1)M_o^4 - \frac{\kappa' h_o^2}{2}(M_o^2-1) \quad ,$$

$$\theta_3 = \frac{h_o h_o' h_o''}{6}\left[\frac{(\gamma+1)M_o^4}{(M_o^2-1)} - 1\right] + \frac{h_o^2 h_o'''(M_o^2-1)}{6}$$

$$+ \frac{\kappa\kappa' h_o^3 (M_o^2-1)}{2} \quad . \qquad \text{(B-7)}$$

$$X_1 = 0 \,,$$

$$X_2 = -\frac{h_0 h_0'}{2} \,,$$

$$X_3 = \frac{\kappa h_0^2 h_0' M_0^2}{6(M_0^2-1)}\left[(\gamma+3)M_0^2-2\right] + \frac{\kappa' h_0^3 (M_0^2-1)}{6} \,,$$

$$X_4 = \frac{h_0 h_0'^3 - h_0^3(M_0^2-1)}{24} - \frac{h_0^2 h_0' h_0''}{24(M_0^2-1)}\left[(\gamma+4)M_0^4 - 7M_0^2 + 4\right]$$

$$- \frac{\kappa\kappa' h_0^4 (M_0^4-1)}{8} \,. \qquad \text{(B-8)}$$

$$Y_1 = h_0 \,,$$

$$Y_2 = -\frac{\kappa h_0^2}{2}(M_0^2-1) \,,$$

$$Y_3 = \frac{h_0}{6}\left[h_0 h_0''(M_0^2-1) - h_0'^2\right] \,,$$

$$Y_4 = -\frac{\kappa h_0^2 h_0'^2}{24(M_0^2-1)^2}\left[\gamma(\gamma+1)M_0^8 - (2\gamma^2+3\gamma+5)M_0^6 + 12M_0^4 - 12M_0^2 + 4\right]$$

$$- \frac{\kappa h_0^3 h_0''}{6}\left[(\gamma+1)M_0^4 - M_0^2 + 1\right]$$

$$- \frac{\kappa' h_0^3 h_0'}{24}\left[(\gamma+1)M_0^4 - 3M_0^2 + 3\right]$$

$$- \frac{\kappa'' h_0^4 (M_0^2-1)^2}{24} \,. \qquad \text{(B-9)}$$

Another series needed is that for the pressure p/p_o, equation (2.34). After multiplication of series (B-3) and equation (2.39), one applies the binomial theorem to get

$$\frac{p}{p_o} = 1 - \gamma M_o^2 q_1 \eta - \gamma M_o^2 q_2 \eta^2 - \gamma M_o^2 [q_3 - (M_o^2 - 1) q_1 q_2] \eta^3 \ . \qquad \text{(B-10)}$$

APPENDIX C

SERIES EXPANSION OF DIFFERENTIAL EQUATION OF PATCHING MACH LINE

Starting with equation (2.54) and expanding $\tan\Theta$ and $(1 + \kappa y)$ into η-series as well as the partials of

$$dx = \frac{\partial x}{\partial \xi} d\xi + \frac{\partial x}{\partial \eta} d\eta \qquad \text{and} \qquad dy = \frac{\partial y}{\partial \xi} d\xi + \frac{\partial y}{\partial \eta} d\eta$$

one gets with equations (2.37), (2.38), and (2.40)

$$\begin{aligned}
&\Big[1 - \{\Theta_1 \tan\beta\}\eta + \{x_2' - \kappa y_1 \Theta_1 \tan\beta - \Theta_2 \tan\beta\}\eta^2 \\
&\quad + \{x_3' + \kappa y_1 x_2' + \kappa y_3 - x_2' \Theta_1 \tan\beta - \kappa y_1 \Theta_2 \tan\beta - (\Theta_3 + \tfrac{\Theta_1^3}{3})\tan\beta\}\eta^3\Big] d\xi \\
&+ \Big[2x_2\eta + \{3x_3 + 2\kappa y_1 x_2 - 2x_2 \Theta_1 \tan\beta\}\eta^2 \\
&\quad + \{4x_4 + 3\kappa y_1 x_3 - (3x_3 + 2\kappa y_1 x_2)\Theta_1 \tan\beta - 2x_2 \Theta_2 \tan\beta\}\eta^3\Big] d\eta \\
&+ \Big[\{y_1' \tan\beta\}\eta + \{y_2' \tan\beta + \Theta_1 y_1'\}\eta^2 \\
&\quad + \{y_3' \tan\beta + \Theta_1 y_2' + \Theta_2 y_1'\}\eta^3\Big] d\xi \\
&+ \Big[y_1 \tan\beta + \{2y_2 \tan\beta + y_1 \Theta_1\}\eta + \{3y_3 \tan\beta + 2y_2 \Theta_1 + y_1 \Theta_2\}\eta^2 \\
&\quad + \{4y_4 \tan\beta + 3y_3 \Theta_1 + 2y_2 \Theta_2 + y_1 \Theta_3 + y_1 \tfrac{\Theta_1^3}{3}\}\eta^3\Big] d\eta \\
&= 0 \; . \qquad (C\text{-}1)
\end{aligned}$$

This equation already includes the fact that $\kappa^2 = x_1 = 0$.

Next the term $\tan\beta$ will be expressed in terms of q/q_o and its series. From equations (2.53) and (2.32) (dropping the subscripts $_o$)

$$\tan^2\beta = M^2 - 1 = \frac{(\gamma+1)\left\{\left(\frac{q_o}{q^*}\right)^2\left(\frac{q}{q_o}\right)^2 - 1\right\}}{(\gamma+1) - (\gamma-1)\left(\frac{q_o}{q^*}\right)^2\left(\frac{q}{q_o}\right)^2} \quad . \quad \text{(C-2)}$$

Substitute equation (2.39), expand binomially and collect terms to get

$$\tan^2\beta \doteq (M_o^2-1)\left[1 + \frac{(\gamma-1)M_o^4 + 2M_o^2}{M_o^2-1}\left\{q_1\eta + q_2\eta^2 + \left[q_3 + \{1+2(\gamma-1)M_o^2\}q_1q_2\right]\eta^3\right\}\right] \quad . \quad \text{(C-3)}$$

Before substituting $\tan\beta$ into equation (C-1), it is convenient to solve equation (C-1) for $\frac{d\eta}{d\xi}$ with $\tan\beta$ retained. It will be seen that all $\tan\beta$ - terms collect to a single $\tan^{-1}\beta$ - term, which from (C-3) becomes

$$\tan^{-1}\beta = \frac{1}{\sqrt{M_o^2-1}}\left[1 - \frac{(\gamma-1)M_o^4 + 2M_o^2}{M_o^2-1}\left\{q_1\eta + q_2\eta^2 + \left[q_3 + \left\{1+2(\gamma-1)M_o^2 - \frac{3(\gamma-1)M_o^4 + 6M_o^2}{M_o^2-1}\right\}q_1q_2\right]\eta^3\right\}\right] \quad . \quad \text{(C-4)}$$

After carrying out the substitutions of equations (B-6), (B-7), (B-8), (B-9), and (C-4) into equation (C-1), solved for $\frac{d\eta}{d\xi}$, one gets equation (2.55).

BIBLIOGRAPHY

1. Puckett, A. E., Design and Operation of a 12" Supersonic Wind Tunnel, I. A. S. preprint No. 160, July, 1948.
2. Murphy, J. S. and Buning, H., Theory and Design of A Variable Mach Number Corner Nozzle, University of Michigan, Engineering Research Institute, Report WTM-221, February, 1952.
3. Foelsch, K. A., A New Method of Designing Two-Dimensional Laval Nozzles for a Parallel and Uniform Jet, JPL-GALCIT Publication No. 3, pp. 156-169, March, 1946.
4. Foelsch, K. A., The Analytical Design of an Axially Symmetric Laval Nozzle for a Parallel and Uniform Jet, Journ. I. A. S., Vol. 16, No. 3, March, 1944.
5. Friedrichs, K. O. et al, Theoretical Studies on the Flow Through Nozzles and Related Problems, AMP Report No. 82.1R AMG-NYU No. 43 (OSRD 3591) April, 1949.
6. Friedrichs, K. O. et al, On Supersonic Compressors and Nozzles, AMP Report No. 822R, AMG-NYU No. 77 (OSRD 4416), October, 1944.
7. Nilson, E., Design of an Inlet for a Two-Dimensional Supersonic Nozzle, Meteor Report UAC-13, December, 1947.
8. Nilson, E., Analytical Correction of a Two-Dimensional Nozzle for Uniform Exhaust Flow, Meteor Report UAC-15, January, 1948.

9. Lighthill, M. J., The Hodograph Transformation in Trans-Sonic Flow, Part I, Symmetrical Channels, Royal Soc. Proc. Series A-191, pp. 323-341, 1947.

10. Goldstein, S., Modern Developments in Fluid Dynamics, Clarendon Press.

11. Frost, R. C., Nozzle Design Considerations, University of Michigan Supersonic Wind Tunnel, Report WTM-188 (unpublished), October, 1950.

12. Görtler, H., Zum Uebergang von Unterschall - zu Ueberschallgeschwindigkeiten in Duesen, ZAMM, Vol. 19, No. 6, pp. 325-337, December, 1939.

13. Sauer, R., General Characteristics of Flow Through Nozzles at Near Critical Speeds, NACA T.M. 1147, June, 1947.

14. Frost, R. C. and Liepman, H. P., Supersonic Nozzles with Continuous Wall Curvature, Reader's Forum, Journ. I. A. S., Vol. 19, No. 10, p. 716, October, 1952.

15. Evvard, J. C. and Marcus, L. E., Achievement of Continuous Wall Curvature in Design of Two-Dimensional Symmetric Supersonic Nozzles, NACA T.N. No. 2616, January, 1952.

16. Kuethe, A. M. and Schetzer, J. D., Foundations of Aerodynamics, John Wiley and Sons, Inc., 1950.

17. Handbook of Supersonic Aerodynamics, Vol. I, Navord Report 1488, p. 497, April, 1950.

18. Tucker, M., Approximate Turbulent Boundary-Layer Development in Plane Compressible Flow along Thermally Insulated Surfaces with Application to Supersonic Tunnel Contour Correction, NACA T.N. 2045, March, 1950.

19. Tucker, M., Approximate Calculation of Turbulent Boundary Layer Development in Compressible Flow, NACA T.N. 2337, April, 1951.